



1         **Quantifying the role of moss in terrestrial ecosystem carbon dynamics in**  
2                                     **northern high-latitudes**

3                                     Junrong Zha and Qianlai Zhuang

4    Department of Earth, Atmospheric, and Planetary Sciences and Department of Agronomy,  
5    Purdue University, West Lafayette, IN 47907, USA

6    Correspondence: Qianlai Zhuang ([qzhuang@purdue.edu](mailto:qzhuang@purdue.edu))

7

8    **Key words: moss, carbon dynamics, Earth System Modeling, terrestrial ecosystems, Arctic**

9

10

11

12

13

14

15

16

17

18



19 **Abstract**

20 **In addition to woody and herbaceous plants, mosses are ubiquitous in northern terrestrial**  
21 **ecosystems, which play an important role in regional carbon, water and energy cycling.**  
22 **Current global land surface models without considering moss may bias the quantification**  
23 **of the regional carbon dynamics. Here we incorporate moss into a process-based**  
24 **biogeochemistry model, the Terrestrial Ecosystem Model (TEM 5.0), as a new plant**  
25 **functional type to develop a new model (TEM\_Moss). The new model explicitly quantifies**  
26 **the interactions between higher plants and mosses and their competition for energy, water,**  
27 **and nutrient. Compared to the estimates using TEM 5.0, the new model estimates that the**  
28 **regional terrestrial soils store 132.7 Pg more C at present day, and will store 157.5 Pg and**  
29 **179.1 Pg more C under the RCP 8.5 and RCP 2.6 scenarios, respectively, by the end of the**  
30 **21<sup>st</sup> century. Ensemble regional simulations forced with different parameters for the 21<sup>st</sup>**  
31 **century with TEM\_Moss predict that the region will accumulate 161.1±142.1 Pg C under**  
32 **the RCP 2.6 scenario, and 186.7±166.1 Pg C under the RCP 8.5 scenario over the century.**  
33 **Our study highlights the necessity of coupling moss into Earth System Models to**  
34 **adequately quantify terrestrial carbon-climate feedbacks in the Arctic.**

35

36

37

38

39



## 40 1. Introduction

41 Northern high latitude ecosystems occupy about 30% of global terrestrial carbon (C) in  
42 soils and plants (Allison and Treseder, 2008; Jobbágy and Jackson, 2000; Kasischke, 2000;  
43 Tarnocai et al., 2009; Hugelius et al., 2014), and contain 1024 Pg soil organic carbon from 0 to 3  
44 m depth (Treseder et al., 2016; Schuur et al., 2008). This large amount of carbon is potentially  
45 responsive to ongoing global warming (McGuire et al., 1995; Melillo et al., 1993; McGuire and  
46 Hobbie, 1997), which is especially pronounced at high latitudes (Treseder et al., 2016; IPCC,  
47 2014). Thus, explicit investigation of carbon-climate feedback is important (Wieder et al., 2013;  
48 Bond-Lamberty and Thomson, 2010).

49 Ecosystem models are important tools for understanding the role of boreal ecosystems in  
50 carbon-climate feedbacks (Bond-Lamberty et al., 2005; Chadburn et al., 2017; Zhuang et al.,  
51 2002; Treseder et al., 2016). Process-based biogeochemical models such as TEM (Hayes et al.,  
52 2014; Raich et al., 1991; Melillo et al., 1993; McGuire et al., 1992; Zhuang et al., 2001, 2002,  
53 2010, 2013), Biome-BGC (Running and Coughlan, 1988; Bond-Lamberty et al., 2007), and  
54 Biosphere Energy Transfer Hydrology scheme (BETHY) (Knorr, 2000) are increasingly  
55 employed to simulate current and future carbon dynamics. Those models estimate carbon  
56 dynamics by simulating processes such as photosynthesis, respiration, nitrogen competition,  
57 evapotranspiration and soil decomposition (Bond-Lamberty et al., 2005; Zhuang et al., 2015).  
58 The results from these models are influenced by components and processes that are built into the  
59 model (Turetsky et al., 2012; Oreskes et al., 1994). However, whether boreal forests act as a  
60 carbon sink or source have not yet reached a consensus due to a number of model limitations  
61 (Cahoon et al., 2012; Hayes et al., 2011; Todd-Brown et al., 2013).



62           One limitation is that ecosystems models often ignore some important components such  
63 as understory processes that play crucial roles in biogeochemical cycles (Zhuang et al., 2002;  
64 Treseder et al., 2011; Bond-Lamberty et al., 2005). For instance, mosses are ubiquitous in  
65 northern ecosystems, and show a pattern of increasing abundance with increasing latitude  
66 (Turetsky et al., 2012; Jägerbrand et al., 2006). Their functional traits, including tolerance to  
67 drought and a broad response of net assimilation rates to temperature, allow them to persist in  
68 high-latitude regions (Kallio and Heinonen, 1975; Harley et al., 1989). The activities of moss  
69 that are related to water, nutrient, and energy may influence several ecosystem processes such as  
70 permafrost formation and thaw, peat accumulation, soil decomposition and net primary  
71 productivity (NPP) (Turetsky et al., 2012; Nilsson and Wardle, 2005). Mosses can have positive  
72 or negative interactions with vascular plants (Skre and Oechel, 1979; Turetsky et al., 2010). On  
73 the one hand, mosses compete with vascular plants for available nutrients, negatively affecting  
74 vascular plant productivity (Skre and Oechel, 1979; Gornall et al., 2011; Turetsky et al., 2012).  
75 Besides, a thick moss cover can form an environment with water logging or low oxygen supply,  
76 which is common in high-latitude regions (Skre and Oechel, 1979; Cornelissen et al., 2007). The  
77 moss cover prevents absorbed solar heat from being conducted down into the soil, and tends to  
78 decrease soil temperature in summer. Therefore, soil decomposition rates can be affected since  
79 they are mediated by soil temperature, which will further influence growth of vascular plants  
80 (Gornall et al., 2007). On the other hand, some species of mosses can serve as an important  
81 source of nitrogen because of their ability of facilitating biological nitrogen fixation and their  
82 low nitrogen-use efficiency (Basilier, 1979; DeLuca et al., 2007; Markham, 2009; Kip et al.,  
83 2011). Thus, mosses can also exert positive effects on plant growth due to their regulation on  
84 nitrogen availability for vascular plants (Hobbie et al., 2000; Gornall et al., 2007). It is gradually



85 recognized that mosses can have comparable influences on high-latitude ecosystems to vascular  
86 plants, due to their large density and essential function in plant competition, soil climate, and  
87 carbon and nutrient cycling (Longton, 1988; Lindo and Gonzalez, 2010; Okland, 1995; Pharo  
88 and Zartman, 2007). They can on average contribute 20% of aboveground NPP in boreal forests  
89 (Turetsky et al., 2010), and their annual NPP may reach as high as  $350 \text{ g C m}^{-2}$  in some regions  
90 in the Arctic (Pakarinen and Vitt 1973), even exceed that of vascular plants (Oechel and Collins,  
91 1976; Clarke et al., 1971). Thus, ignorance of mosses, the keystone species of boreal ecosystems,  
92 can pose large biases in model predictions and limit the utility of models. To date, a number of  
93 ecosystem models have already included moss activities to explore the response of moss to  
94 disturbance (Bond-Lamberty et al., 2007; Euskirchen et al., 2009; Frohking et al., 2010, Wania et  
95 al., 2009, Chadburn et al., 2015, Porada et al., 2016, Druel et al., 2017), or improve model  
96 prediction of carbon dynamics (Bond-Lamberty et al., 2005). However, the potential role of  
97 moss in the regional carbon dynamics in northern high latitudes has been slowly evaluated by  
98 considering the interactions between moss and higher plant, especially with respect to their  
99 competition for water, nutrient and energy.

100 This study developed a new version of Terrestrial Ecosystem Model (Raich et al., 1991;  
101 McGuire et al., 1992; Zhuang et al., 2001, 2002, 2010, 2013, 2015), hereafter referred to as  
102 TEM\_Moss, by explicitly considering moss impacts on terrestrial ecosystem carbon dynamics.  
103 The interactions and competition of water, energy and nutrient between higher plants and mosses  
104 are explicitly modeled. The verified TEM\_Moss and previous TEM were compared against the  
105 observed data of ecosystem carbon, soil temperature and moisture dynamics. Both models were  
106 then used to analyze the regional carbon dynamics in northern high latitudes (north of  $45^\circ \text{N}$ )  
107 during the 20<sup>th</sup> and 21<sup>st</sup> centuries.



108 **2. Methods**

109 **2.1 Overview**

110 First, we briefly describe how we developed the TEM\_Moss by modifying the previous  
111 TEM 5.0 to consider their interactions between higher plants and mosses. Second,  
112 parameterization and validation of TEM\_Moss using measured gap-filled carbon flux data and  
113 meteorological data at representative sites is presented. Third, we present how we have applied  
114 both models (TEM\_Moss and TEM 5.0) to the northern high latitudes (above 45 °N) to quantify  
115 regional carbon dynamics during the 20<sup>th</sup> and 21<sup>st</sup> centuries.

116 **2.2 Model description**

117 TEM is a process-based, large-scale biogeochemical model that uses monthly climatic data  
118 and spatially explicit vegetation and soil information to simulate the dynamics of carbon and  
119 nitrogen fluxes and pool sizes of plants and soils (Raich et al., 1991; McGuire et al., 1992; Zhuang  
120 et al., 2010, 2015, 2020). However, in previous versions of TEM, the interactions between mosses  
121 and higher plants on carbon and nitrogen cycling have not been included. Here we developed a  
122 TEM\_Moss model by modifying model structure and incorporating activities of moss into extant  
123 TEM 5.0 (Zhuang et al., 2003). Based on the structure of TEM 5.0, we added carbon and nitrogen  
124 pools and fluxes to simulate activities of moss including photosynthesis, respiration, litterfall and  
125 nutrient and water cycling (Figure 1). Thus, the structure of TEM\_Moss includes the processes of  
126 both higher plants and mosses (Figure 1).

127 In TEM\_Moss, moss photosynthesis ( $GPP_m$ ) is described as a maximum rate, reduced by  
128 influence of photosynthetically active radiation, mean air temperature, mean atmospheric carbon



129 dioxide concentrations, moss moisture, and indirectly, nitrogen availability (Frolking et al., 1996;  
130 Launiainen et al., 2015; Zhuang et al., 2002). For each time step,  $GPP_m$  is calculated as:

$$131 \quad GPP_m = C_{max} * f(PAR) * f(T) * f(w_m) * f([CO_2]) * f(NA) \quad (1)$$

132 where  $C_{max}$  denotes the maximum rate of carbon assimilation by moss (units:  $gC\ m^{-2}mon^{-1}$ ),  
133  $f(PAR)$  is a scalar function that depends on monthly photosynthetically active radiation (PAR),  
134 which is calculated as (Frolking et al., 1996; Launiainen et al., 2015; Kulmala et al., 2011):

$$135 \quad f(PAR) = \frac{PAR}{b+PAR} \quad (2)$$

136 where  $b$  (units:  $\mu mol\ m^{-2}\ s^{-1}$ ) is the half saturation constant for PAR use by moss as indicated by  
137 the Michaelis–Menten kinetic.

138 The temperature effect on moss photosynthesis is modeled as a multiplier (Frolking et al.,  
139 1996; Raich et al., 1991):

$$140 \quad f(T) = \frac{(T-T_{min})*(T-T_{max})}{(T-T_{min})*(T-T_{max})-(T-T_{opt})^2} \quad (3)$$

141 where  $T$  is the monthly mean air temperature (units:  $^{\circ}C$ ), and  $T_{min}$ ,  $T_{max}$ , and  $T_{opt}$  are parameters  
142 (units:  $^{\circ}C$ ) that limit  $f(T)$  to a range of zero to one.

143 The moisture effect is also modeled as a multiplier (Frolking et al., 1996; Raich et al.,  
144 1991):

$$145 \quad f(w_m) = \frac{(w_m-w_{min})*(w_m-w_{max})}{(w_m-w_{min})*(w_m-w_{max})-(w_m-w_{opt})^2} \quad (4)$$

146 where  $w_m$  is moss moisture (units: mm), and  $w_{min}$ ,  $w_{max}$ , and  $w_{opt}$  are related parameters (units:  
147 mm) that limit  $f(w_m)$  to a range of zero to one.



148  $f([\text{CO}_2])$  is also a scalar function that depends on monthly mean atmospheric carbon  
149 dioxide concentration (Zhuang et al., 2002; Raich et al., 1991):

$$150 \quad f([\text{CO}_2]) = \frac{[\text{CO}_2]}{k_m + [\text{CO}_2]} \quad (5)$$

151 where  $[\text{CO}_2]$  (units:  $\mu\text{L/L}$ ) represents monthly mean atmospheric carbon dioxide concentration,  
152 the  $k_m$  (units:  $\mu\text{L/L}$ ) is the internal  $\text{CO}_2$  concentration at which moss C assimilation proceeds at  
153 one-half its maximum rate.

154 The function  $f(\text{NA})$  models the limiting effects of plant nitrogen status on GPP (McGuire  
155 et al., 1992; Zhuang et al., 2002), which is a unitless multiplier.

156 Meanwhile, in TEM\_Moss, we defined the moss respiration rate ( $R_m$ ) as a function of  
157 moss respiration rate at 10 °C, moss respiration temperature sensitivity which was expressed as a  
158  $Q_{10}$  function, and moss moisture (Launiainen et al., 2015; Frohking et al., 1996):

$$159 \quad R_m = R_{10,m} * Q_{10,m}^{\frac{T_m - 10}{10}} * f^*(w_m) \quad (6)$$

160 where  $R_{10,m}$  (units:  $\text{gC m}^{-2}\text{mon}^{-1}$ ) represents the moss respiration rate at 10 °C, the parameter  
161  $Q_{10,m}$  is moss respiration temperature sensitivity,  $T_m$  is moss temperature (°C) and  $w_m$  is moss  
162 moisture (mm).

163 The function  $f^*(w_m)$  denotes the moisture effect on moss respiration. Here we used  
164  $f^*(w_m)$  to distinguish with the function  $f(w_m)$ , which is moisture effect on moss  
165 photosynthesis as mentioned earlier.  $f^*(w_m)$  is defined as (Frohking et al., 1996; Zhuang et al,  
166 2002):

$$167 \quad f^*(w_m) = 1 - \frac{(w_m - w_{\min} - w_{\text{opt},r})^2}{(w_m - w_{\min}) * w_{\text{opt},r} + w_{\text{opt},r}^2} \quad (7)$$





168 where  $w_{opt,r}$  (units: mm) denotes the optimal water content for moss respiration.

169 Besides, the carbon in litter production from mosses to soil ( $L_{C,m}$ ) is modeled as  
170 proportional to moss carbon biomass with a constant ratio (Zhuang et al., 2002):

$$171 \quad L_{C,m} = cfall_m * MOSSC \quad (8)$$

172 where MOSSC denotes the moss carbon biomass, and  $cfall_m$  is the corresponding constant  
173 proportion.

174 Thus, the change of moss carbon pool (MOSSC) can be modeled as:

$$175 \quad \frac{dMOSSC}{dt} = GPP_m - R_m - L_{C,m} \quad (9)$$

176 On the other hand, researches have shown that mosses can uptake substantial inorganic  
177 nitrogen from the bulk soil (Ayres et al., 2006, Fritz et al., 2014). In our model, nitrogen uptake  
178 by moss ( $N_{uptake_m}$ ) is modelled as a function of available soil nitrogen, moss moisture, and  
179 mean air temperature, and the relative amount of energy allocated to N versus C uptake (Zhuang  
180 et al., 2002; Raich et al., 1991):

$$181 \quad N_{uptake_m} = N_{max} * \frac{K_s * N_{av}}{k_n + K_s * N_{av}} * e^{0.0693T} * (1 - A_m) \quad (10)$$

182 Where  $N_{max}$  is the maximum rate of nitrogen uptake by mosses (units:  $gC\ m^{-2}mon^{-1}$ ), and  $N_{av}$   
183 (units:  $g\ m^{-2}$ ) represents available soil nitrogen, which is treated as a state variable in our model.  
184  $k_n$  (units:  $g\ m^{-2}$ ) is the concentration of available soil nitrogen at which nitrogen uptake proceeds  
185 at one-half its maximum rate.  $T$  is the monthly mean air temperature ( $^{\circ}C$ ), and  $A_m$  is a unitless  
186 parameter ranging from 0 to 1, which represents relative allocation of effort to carbon vs.  
187 nitrogen uptake.  $K_s$  is a parameter accounting for relative differences in the conductance of the



188 soil to N diffusion, which can be calculated through moss moisture (Zhuang et al., 2002; Raich et  
189 al., 1991):

$$190 \quad K_s = 0.9 * \left(\frac{w_m}{w_f}\right)^3 + 0.1 \quad (11)$$

191 where  $w_f$  (units: mm) denotes the moss field capacity.

192 The nitrogen in litter production from mosses to soil ( $L_{N,m}$ ) is modeled as proportional to  
193 moss nitrogen biomass with a constant ratio (Zhuang et al., 2002):

$$194 \quad L_{N,m} = nfall_m * MOSSN \quad (12)$$

195 where  $nfall_m$  is the constant proportion to moss nitrogen biomass (MOSSN).

196 Thus, the changes in moss nitrogen pool (MOSSN) can be modeled as:

$$197 \quad \frac{dMOSSN}{dt} = Nuptake_m - L_{N,m} \quad (13)$$

198 At the same time, total carbon and nitrogen in litterfall, and total nitrogen uptake from  
199 soil available nitrogen are changed due to incorporation of mosses:

$$200 \quad Litterfall_C = L_{C,v} + L_{C,m} \quad (14)$$

$$201 \quad Litterfall_N = L_{N,v} + L_{N,m} \quad (15)$$

$$202 \quad Nuptake = Nuptake_v + Nuptake_m \quad (16)$$

203 Where  $L_{C,v}$  and  $L_{N,v}$  are carbon and nitrogen in litter production from higher plants to soil, and  
204  $Nuptake_v$  is nitrogen uptake by higher plants (Raich et al., 1991; Melillo et al., 1993; Zhuang et  
205 al., 2003).



206 Except above equations, other governing equations in TEM 5.0 have not been changed.  
207 More equations of TEM 5.0 have been documented in previous studies (Raich et al., 1991;  
208 McGuire et al., 1992; Zhuang et al., 2003; Zha and Zhuang, 2018).

209 In TEM 5.0, a soil thermal module (STM) simulates soil thermal dynamics considering  
210 the effects of moss thickness, soil moisture, and snowpack (Zhuang et al., 2001, 2002). In STM,  
211 soil profile was treated as a three soil-layer system: (1) a moss plus fibric soil organic layer, (2) a  
212 humic organic soil layer, and (3) a mineral soil layer, and temperature for each layer can be  
213 derived from STM (Zhuang et al., 2001, 2002, 2003). Temperature in moss layer is estimated  
214 with STM.

215 A water balance module (WBM) was also incorporated into TEM 5.0 to simulate soil  
216 hydrologic dynamics (Vörösmarty et al., 1989; Zhuang et al., 2001). The WBM receives  
217 information on precipitation, air temperature, potential evapotranspiration, vegetation, soils and  
218 elevation to predict soil moisture evapotranspiration and runoff (Vörösmarty et al., 1989). The  
219 whole soil was treated as a single profile in WBM (Vörösmarty et al., 1989; Zhuang et al., 2001).  
220 To simulate moss moisture, we added a moss layer on the soil profile by modifying the WBM  
221 (Figure 2). Similar to soil moisture, moss moisture is also treated as a state variable in the revised  
222 WBM, which is modeled as:

$$223 \quad \frac{dw_m}{dt} = \text{snowfall} + \text{rainfall} - \text{percolation} - \text{moss evapotranspiration} \quad (17)$$

224 where the term “percolation” denotes the percolation from moss, which is the sum of rainfall  
225 percolation and snowmelt percolation from moss. We assume that there is no runoff from moss  
226 layer.

227 Accompanied by the above equation, changes in soil water (SM) is modified as:



228 
$$\frac{dSM}{dt} = \text{percolation} - \text{rain excess} - \text{snow excess} - \text{plant evapotranspiration} \quad (18)$$

229 Calculations for these water fluxes regarding higher plants were not changed. More details about  
230 an earlier version of WBM were described in Vörösmarty et al. (1989) and Zhuang et al. (2001).

### 231 **2.3 Model parameterization and validation**

232 The newly introduced parameters that are associated with moss activities were documented  
233 in Table 1. We parameterized the TEM\_Moss for six representative ecosystem types in northern  
234 high latitudes with gap-filled monthly net ecosystem productivity (NEP,  $\text{gCm}^{-2}\text{mon}^{-1}$ ) data from  
235 the AmeriFlux network (Davidson et al., 2000). We assumed that the moss types are associated  
236 with the representative ecosystem types, which means we tuned the moss-related parameters for  
237 the six representative ecosystem types. Except for the moss-related parameters, other parameters  
238 related to high vegetations are default based on Zha and Zhuang, 2018. The information of six  
239 sites that we chose to calibrate the TEM\_Moss was compiled in Table 2. The parameterization was  
240 conducted using a global optimization algorithm known as SCE-UA (Shuffled complex evolution)  
241 method, which aims to minimize the difference between model simulations and measurements  
242 (Duan et al., 1994). In our calibration, the cost function of the minimization is:

243 
$$\text{Obj} = \sum_{i=1}^k (\text{NEP}_{\text{obs},i} - \text{NEP}_{\text{sim},i})^2 \quad (19)$$

244 Where  $\text{NEP}_{\text{obs},i}$  and  $\text{NEP}_{\text{sim},i}$  are the measured and simulated NEP, respectively.  $k$  is the number  
245 of data pairs for comparison. Fifty independent sets of parameters were converged to minimize the  
246 objective function, and finally the optimized parameters were derived as the mean of these 50 sets  
247 of inversed parameters. We presented the boxplot of parameter posterior distributions at sites  
248 chosen for calibration (Figure 4). At the same time, the results of model parameterization were  
249 shown in Figure 3. Besides these parameters related to moss, all other parameters use their default



250 values in TEM 5.0 (Zhuang et al., 2010, 2015). These optimized parameters were used for model  
251 validation and extrapolation.

252 We verified the TEM\_Moss simulated NEP, soil moisture and soil temperature. First, we  
253 conducted site-level simulations at six sites that contain level-4 gap-filled monthly NEP data from  
254 the AmeriFlux network (Table 3). Site-level monthly gap-filled soil moisture and soil temperature  
255 data were organized from the ORNL DAAC Dataset (<https://daac.ornl.gov/>) to make comparison  
256 with model simulations (Table 4 and Table 5). Local climate data including monthly air  
257 temperature (°C), precipitation (mm), and cloudiness (%) were obtained to drive these model  
258 simulations.

#### 259 **2.4 Regional Extrapolation**

260 Both TEM\_Moss and TEM 5.0 were applied to northern high latitudes (above 45 °N) for  
261 historical (the 20<sup>th</sup> century) and future (the 21<sup>st</sup> century) quantifications on carbon dynamics. For  
262 historical simulations, climatic forcing data including monthly air temperature, precipitation, and  
263 cloudiness and atmospheric CO<sub>2</sub> concentrations during the 20<sup>th</sup> century, were collected from the  
264 Climatic Research Unit (CRU TS3.1) from the University of East Anglia (Harris et al., 2014).  
265 Other ancillary inputs including gridded soil texture (Zhuang et al., 2015), elevation (Zhuang et  
266 al., 2015), and potential natural vegetation (Melillo et al., 1993) were also organized. For future  
267 simulations, two contrasting Intergovernmental Panel on Climate Change (IPCC) climate  
268 scenarios (RCP 2.6 and RCP 8.5) were used to drive the models. The future climate forcing data  
269 and atmospheric CO<sub>2</sub> concentrations during the 21<sup>st</sup> century under these two climate change  
270 scenarios were derived from the HadGEM2-ESmodel, which is a member of CMIP5project213  
271 (<https://esgf-node.llnl.gov/search/cmip5/>, January 2017).



272 Simulations were conducted at a spatial resolution of  $0.5^\circ$  latitude  $\times$   $0.5^\circ$  longitude (Zhuang  
273 et al., 2001, 2002). A spin-up was run to reach an equilibrium for each pixel, and the values of state  
274 variables at equilibrium were treated as initial values for transient simulations (McGuire et al.,  
275 1992). Specifically, we chose the first 30 years in the whole 100-year climatic forcing data to spin-  
276 up the models when conducting historical and future simulations. For each of the simulations, net  
277 primary production (NPP), heterotrophic respiration ( $R_H$ ), and net ecosystem production (NEP)  
278 were analyzed. We denoted that a positive NEP represents a  $\text{CO}_2$  sink from the atmosphere to  
279 terrestrial ecosystems, while a negative value represents a source of  $\text{CO}_2$  from terrestrial  
280 ecosystems to the atmosphere.

281 In these simulations, for each pixel, we assumed its moss distribution area is the same as  
282 the higher plant distribution. The total carbon uptake/emission of mosses in a pixel are calculated  
283 as the multiplication of pixel area with the carbon fluxes such as NEP (units:  $\text{gC m}^{-2} \text{ month}^{-1}$ ).  
284 Moss-related parameters for representative ecosystems are calibrated (Fig. 4 and Table 1) or  
285 obtained from previous model parameterization and the rest of model parameters are default from  
286 Zha and Zhuang (2018).

### 287 3. Results

#### 288 3.1 Model Validation

289 TEM\_Moss was able to reproduce the monthly NEP and performed better than TEM 5.0  
290 at chosen sites, with larger R-square values and smaller RMSE (Figure 5, Table 6). R-square for  
291 TEM\_Moss reached 0.94 at Bartlett Experimental Forest site and 0.72 at Ivotuk site (Table 6). R-  
292 square values for TEM 5.0 showed a similar pattern, reaching 0.91 and with minimum value of  
293 0.43 at Bartlett Experimental Forest and Ivotuk sites, respectively (Table 6). Except for Ivotuk



294 site, R-squares for TEM\_Moss are all higher than 0.8 at the chosen sites, while most R-squares  
295 for TEM 5.0 are from 0.62 to 0.75 (Table 6). On the other hand, RMSE for TEM\_Moss is lower  
296 than that for TEM 5.0 at each site (Table 6).

297 We presented the comparisons between measured and simulated volumetric soil moisture  
298 (VSM) from TEM\_Moss and TEM 5.0 (Figure 6). Statistical analysis shows that TEM\_Moss  
299 reproduces the soil moisture well with R-squares ranging from 0.51 at US-Bkg to 0.87 at US-Atq  
300 (Table 7). R-squares for TEM\_Moss are substantially higher than that for TEM 5.0 at most  
301 chosen sites, except for US-Atq (Table 7). RMSE for TEM\_Moss is lower than that for TEM 5.0  
302 at each site (Table 7). Similarly, comparisons between measured and simulated soil temperature  
303 at 5 cm depth (ST\_5) from TEM\_Moss and TEM 5.0 indicated that TEM\_Moss can reproduce  
304 the soil temperature with R-squares ranging from 0.81 at US-Ho1 to 0.91 at US-Bkg, while TEM  
305 5.0 reproduces the soil temperature with R-squares ranging from 0.69 at BE-Vie to 0.89 at US-  
306 Bkg (Figure 7; Table 8). Although R-squares for both models are relatively high and RMSE for  
307 them are relatively low, TEM\_Moss still shows higher R-squares and lower RMSE than TEM  
308 5.0 (Table 8).

### 309 **3.2 Regional carbon dynamics during the 20<sup>th</sup> century**

310 Both TEM\_Moss and TEM 5.0 were used to simulate northern high-latitude regional  
311 carbon balance during the 20<sup>th</sup> century (Figure 8). Higher NEP was correlated with the  
312 combination of relatively higher NPP and lower heterotrophic respiration ( $R_H$ ). TEM\_Moss  
313 indicated that the northern high latitudes acted as a carbon sink of 221.9 Pg with an inter-annual  
314 standard deviation of 0.31 PgC yr<sup>-1</sup> during the 20<sup>th</sup> century, which is 132.7 Pg larger than 89.2 Pg  
315 simulated by TEM 5.0 (Figure 8). The simulated NEP by TEM\_Moss ranges from 1.38 PgC yr<sup>-1</sup>  
316 to 3.05 PgC yr<sup>-1</sup>, while the range by TEM 5.0 was from 0.11 PgC yr<sup>-1</sup> to 1.75 PgC yr<sup>-1</sup> (Figure 8).



317 The patterns of the simulated NEP from two models were similar, both showing a general  
318 increasing trend throughout the 20<sup>th</sup> century (Figure 8). By 2000, the TEM\_Moss simulation  
319 indicated that the northern high-latitude region stored 3.05 PgC yr<sup>-1</sup>, which is more than twice as  
320 the storage estimated by TEM 5.0 (1.33 PgC yr<sup>-1</sup>, Figure 8). Both models indicated that carbon  
321 uptake by the northern ecosystems during the second half of the 20<sup>th</sup> century was higher than the  
322 first half for most part of the region, and only a small portion of the region lost carbon in last  
323 century (Figure 9).

324 Simulated total NPP by TEM\_Moss was 9.6 PgC yr<sup>-1</sup>, ranging from 8.52 PgC yr<sup>-1</sup> to  
325 10.65 PgC yr<sup>-1</sup> in the 20<sup>th</sup> century, with 1.69 PgC yr<sup>-1</sup> of moss NPP and 7.93 PgC yr<sup>-1</sup> of higher  
326 plant NPP (Figure 8). Moss NPP ranges from 1.23 PgC yr<sup>-1</sup> to 2.14 PgC yr<sup>-1</sup> and the ratio of moss  
327 NPP to higher plant NPP is 0.21 (Figure 8). TEM 5.0 estimated 0.8 PgC yr<sup>-1</sup> lower total NPP than  
328 TEM\_Moss, but 0.87 PgC yr<sup>-1</sup> higher NPP for higher plants (Figure 8). On the other hand,  
329 average heterotrophic respiration in the 20<sup>th</sup> century was 7.38 PgC yr<sup>-1</sup> and all years were within  
330 about 5% of this value (Figure 8). TEM 5.0 projected 0.53 PgC yr<sup>-1</sup> higher R<sub>H</sub> than TEM\_Moss  
331 (7.91 PgC yr<sup>-1</sup>, Figure 8). Overall, TEM\_Moss predicted higher total NPP but lower R<sub>H</sub>, which  
332 jointly caused a pronounced difference in NEP between two models.

333 Both models estimated that soil organic carbon and vegetation carbon were accumulating  
334 continuously in the 20<sup>th</sup> century (Figure 10). TEM\_Moss indicated that regional SOC and VEGC  
335 accumulated 96.3 PgC and 115.2 PgC, respectively, and the carbon uptake by moss was 10.4 Pg  
336 the period (Figure 10, Table 10). As simulated by TEM\_Moss, 43.4%, 51.9% and 4.7% of total  
337 carbon uptake in the region was assimilated to soils, higher plants and mosses, respectively  
338 (Table 10). TEM 5.0 simulated that SOC increased by 31.7 Pg at the end of the 20<sup>th</sup> century,  
339 which is 64.6 PgC less than the value estimated by TEM\_Moss (Table 10). TEM 5.0 estimated





340 57.7 PgC in plants less than the value estimated by TEM\_Moss (57.5 PgC, Table 10). 35.5% and  
341 64.5% of total carbon was as SOC and VEGC, respectively.

### 342 **3.3 Regional carbon dynamics during the 21<sup>st</sup> century**

343 Under the RCP 2.6 scenario, TEM\_Moss simulated NEP of 2.07 PgC yr<sup>-1</sup> with the range  
344 from 0.41 PgC yr<sup>-1</sup> to 3.2 PgC yr<sup>-1</sup>, and the inter-annual standard deviation of 0.59 PgC yr<sup>-1</sup>  
345 during the 21<sup>st</sup> century (Figure 11 (a)). The regional sink shows a decreasing pattern in the 2000s  
346 and then generally increases over the remaining years of the 21<sup>st</sup> century (Figure 11 (a)). For  
347 comparison, TEM 5.0 predicted that the average NEP of 0.28 PgC yr<sup>-1</sup> with the range from -1.48  
348 PgC yr<sup>-1</sup> to 1.69 PgC yr<sup>-1</sup> during the 21<sup>st</sup> century (Figure 11 (a)). Thus, TEM 5.0 projected 179.1  
349 PgC stored in northern ecosystems is less than the estimation from TEM\_Moss in the 21<sup>st</sup>  
350 century. Besides, TEM 5.0 simulated that the regional NEP showed a decreasing trend and the  
351 region fluctuates between sinks and sources during the century (Figure 11 (a)). The spatial  
352 patterns from two models also showed differences. TEM\_Moss indicated that the region  
353 accumulates carbon over this century, while TEM 5.0 simulated that some regions changed from  
354 a carbon sink to a source in the second half of the century (Figure 12 (a)). Simulated regional  
355 NPP by TEM\_Moss ranges from 11.2 to 13.7 PgC yr<sup>-1</sup> with a mean of 12.98 PgC yr<sup>-1</sup> in this  
356 century, while average NPP predicted by TEM 5.0 is 1.46 PgC yr<sup>-1</sup> lower than that value (11.52  
357 PgC yr<sup>-1</sup> (Figure 11(a)). TEM\_Moss simulated NPP has 3.74 PgC yr<sup>-1</sup> from moss and 9.24 PgC  
358 yr<sup>-1</sup> from higher plants, which account for 28.8% and 71.2% of total NPP, respectively (Figure  
359 11(a)). Meanwhile, TEM\_Moss estimated that R<sub>H</sub> is 10.91 PgC yr<sup>-1</sup>, while TEM 5.0 predicted it  
360 as 0.33 PgC yr<sup>-1</sup>, which is higher (Figure 11(a)). Both models projected that soil organic carbon  
361 and vegetation carbon accumulate in this century but with different magnitudes (Figure 13 (a)).  
362 TEM\_Moss predicted that regional SOC and VEGC accumulated 84.7 PgC and 112.6 PgC,



363 respectively, during the 21<sup>st</sup> century, while TEM 5.0 predicted that a smaller increase with 12.1  
364 and 15.5 PgC in SOC and VEGC, respectively (Figure 13 (a), Table 12 (a)). Besides, TEM\_Moss  
365 also predicted an increasing of 9.4 PgC in MOSSC, accounting for 4.5% of the total carbon  
366 uptake in this region (Table 12(a)).

367 Under the RCP 8.5 scenario, TEM\_Moss simulated annual NPP of 13.84 PgC yr<sup>-1</sup> with a  
368 range from 11.09 to 16.94 PgC yr<sup>-1</sup>, which is 1.31 PgC yr<sup>-1</sup> higher than the projection from TEM  
369 5.0 (Figure 11 (b)). Total NPP estimated by TEM\_Moss has 3.84 PgC yr<sup>-1</sup> from moss and 10  
370 PgC yr<sup>-1</sup> from higher plants (Figure 11(b)). Annual R<sub>H</sub> was 11.28 PgC yr<sup>-1</sup> estimated by  
371 TEM\_Moss and 11.54 PgC yr<sup>-1</sup> by TEM 5.0, respectively (Figure 11(b)). Consequently,  
372 TEM\_Moss projected NEP was 2.56 PgC yr<sup>-1</sup> with the inter-annual standard deviation of 0.93  
373 PgC yr<sup>-1</sup> in this century (Figure 11 (b)). NEP ranges from 0.67 PgC yr<sup>-1</sup> to 4.78 PgC yr<sup>-1</sup>  
374 estimated with TEM\_Moss, while from -1.69 PgC yr<sup>-1</sup> to 2.65 PgC yr<sup>-1</sup> with a mean of 0.99 PgC  
375 yr<sup>-1</sup> was estimated by TEM 5.0 (Figure 11 (b)). TEM\_Moss predicted more carbon uptake of  
376 157.5 Pg than TEM 5.0 during the 21<sup>st</sup> century. Both models predicted that NEP showed an  
377 increasing trend during the 21<sup>st</sup> century (Figure 11 (b)). Moreover, similar spatial patterns of  
378 carbon sinks and sources appeared in the projections from two models (Figure 12 (b)). Soil  
379 organic carbon and vegetation carbon shows an increasing trend from both models (Figure 13  
380 (b)). Regional SOC and VEGC increased by 92.5 PgC and 153.6 PgC, respectively by the end of  
381 the 21<sup>st</sup> century predicted by TEM\_Moss. In contrast, the increase of 44.2 PgC and 54.5 PgC of  
382 SOC and VEGC, respectively, was predicted by TEM 5.0 (Figure 13 (b), Table 12 (b)). TEM\_Moss  
383 predicted an increase of 10.1 PgC in MOSSC (Table 12(b)).

#### 384 4. Discussion

##### 385 4.1 The role of moss in the regional carbon dynamics



386  
387           Global warming has been pronounced in recent decades, particularly at high latitudes  
388 (IPCC, 2014; Tape et al., 2006; Stow et al., 2004). An enormous amount of soil organic carbon  
389 stored in northern high-latitude regions (Tarnocai et al., 2009; Schuur et al., 2008) is expected to  
390 affect a broad spectrum of ecological and human systems, and cause rapid changes in the Earth  
391 system when undergoing substantial climate change (Serreze and Francis 2006; Davidson and  
392 Janssens, 2006; McGuire et al., 2009). Improving projections for carbon budget of high latitude  
393 terrestrial ecosystems is essential for understanding global carbon–climate feedbacks (Melillo et  
394 al., 2011; Todd-Brown et al., 2013).

395           Our simulations suggest that mosses play an important role in the regional carbon  
396 dynamics, which is consistent with previous studies (McGuire et al., 2009; Turetsky et al., 2012).  
397 First of all, mosses are productive with carbon assimilation even during low temperature, water  
398 content and irradiance (Kallio and Heinonen, 1975; Harley et al., 1989). For example, mosses  
399 can tolerate drought through physiological responses, such as by suspending metabolism and by  
400 withstanding cell desiccation (Turetsky et al., 2012; Oechel and Van Cleve, 1986). The key  
401 functional traits related to water, nutrient, and thermal tolerances of mosses enable them to fit in  
402 harsh northern conditions (Shetler et al., 2008; Turetsky et al., 2012). Thus, with incorporation of  
403 moss into our models, NPP estimation in our model is improved. Mosses also act as a powerful  
404 competitor with vascular plants for nutrient uptake. Their rapid nutrient acquisition and slow  
405 nutrient loss through slow decomposition may constrain concentrations of plant-available  
406 nitrogen (Hobbie et al., 2000; Turetsky et al., 2010; Oechel and Van Cleve, 1986; Gornall et al.,  
407 2007), which will further decrease NPP of higher plant. Our model results suggested that the  
408 NPP of higher plants considering moss is indeed lower than previous NPP estimates without  
409 considering moss, but the total NPP is larger than before. We estimated that mosses contribute



410 17.6% of NPP in the 20<sup>th</sup> century, and 28.8% and 27.6% in the 21<sup>st</sup> century under the RCP 2.6  
411 and RCP 8.5 scenarios, respectively. This is comparable with the results reported by Turetsky et  
412 al. (2010), which suggested an average contribution of 20% of aboveground NPP from moss in  
413 boreal forests. Frohking et al. (1996) even reported a contribution of 38.4% to total NPP by moss  
414 at a boreal forest site. Moreover, mosses can also influence heterotrophic respiration ( $R_H$ )  
415 through their effects on soil thermal and hydrologic dynamics (Zhuang et al., 2001). With the  
416 layer of moss, soil temperature tends to decrease but soil moisture tends to increase (Oechel and  
417 Van Cleve, 1986), which will further decrease soil respiration in summer. This supports our  
418 results that TEM\_Moss simulated  $R_H$  is lower than that by TEM 5.0. With a combination of  
419 higher NPP and lower  $R_H$ , NEP predicted by TEM\_Moss is larger than that by TEM 5.0. The  
420 two contrasting regional simulations by TEM\_Moss and TEM 5.0 indicated the region is  
421 currently a carbon sink, which is consistent with previous studies (White et al., 2000; McGuire et  
422 al., 2009; Schimel et al., 2001). Our study estimated that regional NEP during the 20<sup>th</sup> century is  
423 2.2 Pg C yr<sup>-1</sup> by TEM\_Moss and 0.89 Pg C yr<sup>-1</sup> by TEM 5.0, respectively. In the 1990s, the  
424 regional sink is projected to be 2.7 and 1.1 Pg C yr<sup>-1</sup> by TEM\_Moss and TEM 5.0 respectively.  
425 Compared with other existing studies, our regional estimates of NEP are within the reasonable  
426 range from other existing studies. McGuire et al. (2009) estimated a land sink of 0.3–0.6 Pg C yr<sup>-1</sup>  
427 for the pan-arctic region for the 1990s, which is closer to our estimation by TEM 5.0 but less  
428 than the projection by TEM\_Moss. The top-down atmospheric analyses indicate that the sink of  
429 pan-arctic region is between 0 and 0.8 Pg C yr<sup>-1</sup> in the 1990s (Menon et al. 2007). Besides,  
430 Schimel et al. (2001) reported an estimation of the northern extratropical NEP is from 0.6 to 2.3  
431 PgC yr<sup>-1</sup> in the late 20<sup>th</sup> century, which is comparable to our estimates. Our simulations also



432 confirmed that mosses and higher plants respond to climate change similarly in terms of their  
433 productivity (Turetsky et al. 2010).

#### 434 **4.2 Model Uncertainty and limitations**

435         There are a number of uncertainty sources in our model simulations. First, the errors in  
436 the observed data will influence our parameterization results, which will bias our regional  
437 estimates of carbon dynamics. Second, climatic driving data are also a source of uncertainty for  
438 historical and future simulations. Third, model assumptions will also induce additional  
439 uncertainties. For instance, we assumed that vegetation distribution will remain unchanged  
440 during the transient simulation. However, vegetation will change in response to warming climate  
441 and disturbances such as fire and insect outbreaks in the region (Hansen et al., 2006), which will  
442 affect carbon budget. Missing potential responses to disturbances in our model shall introduce  
443 additional uncertainties (Soja et al. 2007; Kasischke and Turetsky, 2006).

444         We conducted ensemble regional simulations with 50 sets of parameters to quantify  
445 model uncertainty due to uncertain parameters. The 50 sets of parameters were obtained using  
446 the method in Tang and Zhuang (2008). The ensemble means and the inter-simulation standard  
447 deviations are used to measure the model uncertainty (Figure 14). TEM\_Moss predicted that the  
448 regional cumulative carbon ranges from a carbon loss of 266 Pg C to a carbon sink of 567.3 Pg C  
449 by different ensemble members, with a mean of  $161.1 \pm 142.1$  Pg during the 21<sup>st</sup> century under the  
450 RCP 2.6 scenario. Under the RCP 8.5 scenario, TEM\_Moss predicted that the region acts from a  
451 carbon source of 79.1 Pg C to a carbon sink of 625.9 Pg C, with a mean of  $186.7 \pm 166.1$  Pg  
452 during the 21<sup>st</sup> century (Figure 14).

453         This study took an important step to incorporate moss into an extant ecosystem model  
454 that has not explicitly consider the role of moss and its interactions with higher plants. Our



455 model simulations showed that mosses have strong influences on regional ecosystem carbon  
456 cycling, by affecting the soil thermal, nitrogen availability, and water conditions of terrestrial  
457 ecosystems. However, there are still limitations in our model. First, we did not differentiate  
458 various kinds of mosses because they have their own functional traits. In our model, the moss  
459 types are just differentiated by the vegetation types. The structural and physiological traits of  
460 mosses will differ largely in different moss groups, such as feather moss versus Sphagnum  
461 (Turetsky et al., 2010). In addition, we lack spatially explicit information of moss distribution in  
462 the region, which will lead to a large regional uncertainty of carbon quantification. We assumed  
463 that moss area distribution is the same as its associated vegetation distribution. Another  
464 limitation is that some important physiological traits of moss have not been modeled. For  
465 example, moss abundance may change following shifts in vascular species composition due to  
466 shading or burial by vascular litter (Turetsky et al., 2010; Cornelissen et al., 2007). Furthermore,  
467 disturbance such as wildfires can also influence moss activities.

## 468 **5. Conclusions**

469 This study explicitly incorporated moss into an extant process-based terrestrial ecosystem model  
470 to investigate the carbon dynamics in the Arctic for present day and future. Historical regional  
471 simulations with TEM\_Moss indicated that the region is a carbon sink of 221.9 PgC over the 20<sup>th</sup>  
472 century, and this sink may decrease to 206.7 PgC under the RCP 2.6 scenario or increase to 256.2  
473 PgC under the RCP 8.5 scenario during the 21<sup>st</sup> century. Compared with an earlier version of TEM  
474 that has not explicitly modeled moss, TEM\_Moss projected that the region stored 132.7 Pg more  
475 C over the last century, 179.1 Pg and 157.5 Pg more C under the RCP 2.6 and RCP 8.5 scenarios,  
476 respectively. This study demonstrated that moss activities have large effects on ecosystem soil  
477 thermal, water, and carbon dynamics through their interactions with higher plants. This study



478 highlights the importance of considering the moss dynamics in Earth System Models to adequately  
479 quantify the carbon–climate feedbacks in the Arctic.

## 480 **6. Acknowledgments**

481 This research was supported by an NSF project (IIS-1027955), a DOE project (DE-SC0008092),  
482 and a NASA LCLUC project (NNX09AI26G). We acknowledge the Rosen High Performance  
483 Computing Center at Purdue for computing support. We also acknowledge the World Climate  
484 Research Programme’s Working Group on Coupled Modeling Intercomparison Project CMIP5,  
485 and we thank the climate modeling groups for producing and making available their model  
486 output. The data of this study can be accessed from Purdue Research Repository.

487

## 488 **References**

- 489 Allison, S. D., and Treseder, K. K.: Warming and drying suppress microbial activity and carbon cycling in  
490 boreal forest soils, *Global change biology*, 14, 2898-2909, 10.1111/j.1365-2486.2008.01716.x, 2008.
- 491 Basilier, K.: Moss-associated nitrogen fixation in some mire and coniferous forest environments around  
492 Uppsala, Sweden, *Lindbergia*, 5, 84-88, 1979.
- 493 Ben Bond-Lamberty, S. T. G., Douglas E. Ahl and Peter E. Thornton: Reimplementation of the Biome-  
494 BGC model to simulate successional change, *Tree Physiology*, 25, 413–424, 2005.
- 495 Bond-Lamberty, B., Peckham, S. D., Ahl, D. E., and Gower, S. T.: Fire as the dominant driver of central  
496 Canadian boreal forest carbon balance, *Nature*, 450, 89-92, 10.1038/nature06272, 2007.
- 497 Bond-Lamberty, B., and Thomson, A.: Temperature-associated increases in the global soil respiration  
498 record, *Nature*, 464, 579-582, 10.1038/nature08930, 2010.
- 499 Cahoon, S. M., Sullivan, P. F., Shaver, G. R., Welker, J. M., Post, E., and Holyoak, M.: Interactions  
500 among shrub cover and the soil microclimate may determine future Arctic carbon budgets, *Ecology*  
501 *letters*, 15, 1415-1422, 10.1111/j.1461-0248.2012.01865.x, 2012.
- 502 Chadburn, S. E., Burke, E. J., Cox, P. M., Friedlingstein, P., Hugelius, G., and Westermann, S.: An  
503 observation-based constraint on permafrost loss as a function of global warming, *Nature Climate Change*,  
504 7, 340-344, 10.1038/nclimate3262, 2017.



- 505 Charles J. Vörösmarty, B. M. I., Annette L. Grace, and M. Patricia Gildea: Continental scale models of  
506 water balance and fluvial transport: an application to South America, *Global biogeochemical cycles*, 3,  
507 241-265, 1989.
- 508 Christian Fritz, L. P. M. L., Muhammad Riaz, Leon J. L. van den Berg, Theo J. T.M. Elzenga: Sphagnum  
509 Mosses - Masters of Efficient N-Uptake while Avoiding Intoxication, *PLoS ONE*, 9,  
510 10.1371/journal.pone.0079991, 2014.
- 511 Clarke, G. C. S.: Productivity of Bryophytes in Polar Regions, *Annals of botany*, 35, 99–108, 1971.
- 512 Collins, W. C. O. a. N. J.: Comparative CO<sub>2</sub> exchange patterns in mosses from two tundra habitats at  
513 Barrow, Alaska, *Canadian Journal of Botany*, 54, 1355-1369, 1976.
- 514 Cornelissen, J. H., Lang, S. I., Soudzilovskaia, N. A., and During, H. J.: Comparative cryptogam ecology:  
515 a review of bryophyte and lichen traits that drive biogeochemistry, *Annals of botany*, 99, 987-1001,  
516 10.1093/aob/mcm030, 2007.
- 517 Davidson, E. A., Trumbore, S. E., and Amundson, R.: Soil warming and organic carbon content, *Nature*,  
518 408, 789, 10.1038/35048672, 2000.
- 519 Davidson, E. A., and Janssens, I. A.: Temperature sensitivity of soil carbon decomposition and feedbacks  
520 to climate change, *Nature*, 440, 165-173, 10.1038/nature04514, 2006.
- 521 Davidson, E. A., Janssens, I. A., and Luo, Y.: On the variability of respiration in terrestrial ecosystems:  
522 moving beyond Q<sub>10</sub>, *Global change biology*, 12, 154-164, 10.1111/j.1365-2486.2005.01065.x, 2006.
- 523 DeLuca, T. H., Zackrisson, O., Gentili, F., Sellstedt, A., and Nilsson, M. C.: Ecosystem controls on  
524 nitrogen fixation in boreal feather moss communities, *Oecologia*, 152, 121-130, 10.1007/s00442-006-  
525 0626-6, 2007.
- 526 Duan, Q., Sorooshian, S., and Gupta, V. K.: Optimal use of the SCE-UA global optimization method for  
527 calibrating watershed models, *Journal of Hydrology*, 158, 265-284, 1994.
- 528 E. S. Euskirchen, A. D. M., F. S. Chapin, III, S. Yi, and C. C. Thompson: Changes in vegetation in  
529 northern Alaska under scenarios of climate change, 2003–2100: implications for climate feedbacks,  
530 *Ecological Applications*, 19, 1022–1043, 2009.
- 531 Edward A. G. Schuur, J. B., Josep G. Canadell, Eugenie Euskirchen, Christopher B., Field, S. V. G.,  
532 Stefan Hagemann, Peter Kuhry, Peter M. Lafleur, Hanna Lee, Galina, Mazhitova, F. E. N., Annette Rinke,  
533 Vladimir E. Romanovsky, Nikolay Shiklomanov,, and Charles Tarnocai, S. V., Jason G. Vogel, And Sergei  
534 A. Zimov: Vulnerability of Permafrost Carbon to Climate Change: Implications for the Global Carbon  
535 Cycle, *BioScience*, 58, 701-714, 2008.
- 536 Edward Ayres, R. v. d. W., Martin Sommerkorn, Richard D. Bardgett: Direct uptake of soil nitrogen by  
537 mosses, *Biology Letters*, 2, 286-288, 10.1098/rsbl.2006.0455, 2006.





- 538 Esteban G. Jobbágy, and Jackson, R. B.: The vertical distribution of soil organic carbon and its relation to  
539 climate and vegetation, *Ecological applications*, 10, 423-436, 2000.
- 540 Frolking, S., Roulet, N. T., Tuittila, E., Bubier, J. L., Quillet, A., Talbot, J., and Richard, P. J. H.: A new  
541 model of Holocene peatland net primary production, decomposition, water balance, and peat  
542 accumulation, *Earth System Dynamics*, 1, 1-21, 10.5194/esd-1-1-2010, 2010.
- 543 Gilmanov, T. G., Tieszen, L. L., Wylie, B. K., Flanagan, L. B., Frank, A. B., Haferkamp, M. R., Meyers,  
544 T. P., and Morgan, J. A.: Integration of CO<sub>2</sub> flux and remotely-sensed data for primary production and  
545 ecosystem respiration analyses in the Northern Great Plains: potential for quantitative spatial  
546 extrapolation, *Global Ecology and Biogeography*, 14, 271-292, 10.1111/j.1466-822X.2005.00151.x, 2005.
- 547 Gornall, J. L., Jonsdottir, I. S., Woodin, S. J., and Van der Wal, R.: Arctic mosses govern below-ground  
548 environment and ecosystem processes, *Oecologia*, 153, 931-941, 10.1007/s00442-007-0785-0, 2007.
- 549 Gornall, J. L., Woodin, S. J., Jonsdottir, I. S., and van der Wal, R.: Balancing positive and negative plant  
550 interactions: how mosses structure vascular plant communities, *Oecologia*, 166, 769-782,  
551 10.1007/s00442-011-1911-6, 2011.
- 552 Gough, C. M., Hardiman, B. S., Nave, L. E., Bohrer, G., Maurer, K. D., Vogel, C. S., Nadelhoffer, K. J.,  
553 and Curtis, P. S.: Sustained carbon uptake and storage following moderate disturbance in a Great Lakes  
554 forest, *Ecological Applications*, 23, 1202-1215, 2013.
- 555 Goulden, M. L., Winston, G. C., McMillan, A. M. S., Litvak, M. E., Read, E. L., Rocha, A. V., and Rob  
556 Elliot, J.: An eddy covariance mesonet to measure the effect of forest age on land-atmosphere exchange,  
557 *Global change biology*, 12, 2146-2162, 10.1111/j.1365-2486.2006.01251.x, 2006.
- 558 Hansen, J., Sato, M., Ruedy, R., Lo, K., Lea, D. W., and Medina-Elizade, M.: Global temperature change,  
559 *Proceedings of the National Academy of Sciences of the United States of America*, 103, 14288-14293,  
560 10.1073/pnas.0606291103, 2006.
- 561 Harris, I., Jones, P. D., Osborn, T. J., and Lister, D. H.: Updated high-resolution grids of monthly climatic  
562 observations - the CRU TS3.10 Dataset, *International Journal of Climatology*, 34, 623-642,  
563 10.1002/joc.3711, 2014.
- 564 Hayes, D. J., McGuire, A. D., Kicklighter, D. W., Gurney, K. R., Burnside, T. J., and Melillo, J. M.: Is the  
565 northern high-latitude land-based CO<sub>2</sub> sink weakening?, *Global Biogeochemical Cycles*, 25, n/a-n/a,  
566 10.1029/2010gb003813, 2011.
- 567 Hayes, D. J., Kicklighter, D. W., McGuire, A. D., Chen, M., Zhuang, Q., Yuan, F., Melillo, J. M., and  
568 Wullschlegel, S. D.: The impacts of recent permafrost thaw on land-atmosphere greenhouse gas  
569 exchange, *Environmental Research Letters*, 9, 045005, 10.1088/1748-9326/9/4/045005, 2014.



- 570 Hiller, R. V., McFadden, J. P., and Kljun, N.: Interpreting CO<sub>2</sub> Fluxes Over a Suburban Lawn: The  
571 Influence of Traffic Emissions, *Boundary-Layer Meteorology*, 138, 215-230, 10.1007/s10546-010-9558-  
572 0, 2010.
- 573 Hugelius, G., Strauss, J., Zubrzycki, S., Harden, J. W., Schuur, E. A. G., Ping, C. L., Schirrmeister, L.,  
574 Grosse, G., Michaelson, G. J., Koven, C. D., amp, apos, Donnell, J. A., Elberling, B., Mishra, U., Camill,  
575 P., Yu, Z., Palmtag, J., and Kuhry, P.: Estimated stocks of circumpolar permafrost carbon with quantified  
576 uncertainty ranges and identified data gaps, *Biogeosciences*, 11, 6573-6593, 10.5194/bg-11-6573-2014,  
577 2014.
- 578 Jägerbrand, A. K., Lindblad, K. E. M., Björk, R. G., Alatalo, J. M., and Molau, U.: Bryophyte and Lichen  
579 Diversity Under Simulated Environmental Change Compared with Observed Variation in Unmanipulated  
580 Alpine Tundra, *Biodiversity and Conservation*, 15, 4453-4475, 10.1007/s10531-005-5098-1, 2006.
- 581 Jenkins, J. P., Richardson, A. D., Braswell, B. H., Ollinger, S. V., Hollinger, D. Y., and Smith, M. L.:  
582 Refining light-use efficiency calculations for a deciduous forest canopy using simultaneous tower-based  
583 carbon flux and radiometric measurements, *Agricultural and Forest Meteorology*, 143, 64-79,  
584 10.1016/j.agrformet.2006.11.008, 2007.
- 585 Kasischke, E. S.: Boreal ecosystems in the global carbon cycle. In *Fire, climate change, and carbon*  
586 *cycling in the boreal forest*, *Ecological Studies (Analysis and Synthesis)*, 138, 19-30,  
587 [https://doi.org/10.1007/978-0-387-21629-4\\_2](https://doi.org/10.1007/978-0-387-21629-4_2), 2000.
- 588 Kasischke, E. S., and Turetsky, M. R.: Recent changes in the fire regime across the North American  
589 boreal region—Spatial and temporal patterns of burning across Canada and Alaska, *Geophysical Research*  
590 *Letters*, 33, 10.1029/2006gl025677, 2006.
- 591 Kip, N., Ouyang, W., van Winden, J., Raghoebarsing, A., van Niftrik, L., Pol, A., Pan, Y., Bodrossy, L.,  
592 van Donselaar, E. G., Reichart, G. J., Jetten, M. S., Damste, J. S., and Op den Camp, H. J.: Detection,  
593 isolation, and characterization of acidophilic methanotrophs from Sphagnum mosses, *Applied and*  
594 *environmental microbiology*, 77, 5643-5654, 10.1128/AEM.05017-11, 2011.
- 595 Knorr, W.: Annual and interannual CO<sub>2</sub> exchanges of the terrestrial biosphere: process-based simulations  
596 and uncertainties, *Global Ecology and Biogeography*, 9, 225-252, 2000.
- 597 L. Kulmala, J. P., P. Hari and T. Vesala: Photosynthesis of ground vegetation in different aged pine forests:  
598 Effect of environmental factors predicted with a process-based model, *Journal of Vegetation Science*, 22,  
599 96–110, 2011.
- 600 Launiainen, S., Katul, G. G., Lauren, A., and Kolari, P.: Coupling boreal forest CO<sub>2</sub>, H<sub>2</sub>O and energy  
601 flows by a vertically structured forest canopy – Soil model with separate bryophyte layer, *Ecological*  
602 *Modelling*, 312, 385-405, 10.1016/j.ecolmodel.2015.06.007, 2015.



- 603 Lindo, Z., and Gonzalez, A.: The Bryosphere: An Integral and Influential Component of the Earth's  
604 Biosphere, *Ecosystems*, 13, 612-627, 10.1007/s10021-010-9336-3, 2010.
- 605 Longton, R. E.: Adaptations and strategies of polar bryophytes, *Botanical Journal of the Linnean Society*,  
606 98, 253-268, 1988.
- 607 Markham, J. H.: Variation in moss-associated nitrogen fixation in boreal forest stands, *Oecologia*, 161,  
608 353-359, 10.1007/s00442-009-1391-0, 2009.
- 609 McEwing, K. R., Fisher, J. P., and Zona, D.: Environmental and vegetation controls on the spatial  
610 variability of CH<sub>4</sub> emission from wet-sedge and tussock tundra ecosystems in the Arctic, *Plant and soil*,  
611 388, 37-52, 10.1007/s11104-014-2377-1, 2015.
- 612 McGuire, A. D., Melillo, J. M., Joyce, L. A., Kicklighter, D. W., Grace, A. L., III, B. M., and Vorosmarty,  
613 C. J.: Interactions between carbon and nitrogen dynamics in estimating net primary productivity for  
614 potential vegetation in North America, *Global Biogeochemical Cycles*, 6, 101-124, 1992.
- 615 McGuire, A. D., Melillo, J. M., Kicklighter, D. W., and Joyce, L. A.: Equilibrium responses of soil carbon  
616 to climate change: Empirical and process-based estimates, *Journal of Biogeography*, 785-796, 1995.
- 617 McGuire, A. D., and Hobbie, J. E.: Global climate change and the equilibrium responses of carbon  
618 storage in arctic and subarctic regions, In *Modeling the Arctic system: A workshop report on the state of*  
619 *modeling in the Arctic System Science program*, 53-54, 1997.
- 620 McGuire, A. D., Anderson, L. G., Christensen, T. R., Dallimore, S., Guo, L., Hayes, D. J., Heimann, M.,  
621 Lorenson, T. D., Macdonald, R. W., and Roulet, N.: Sensitivity of the carbon cycle in the Arctic to climate  
622 change, *Ecological Monographs*, 79, 523-555, 2009.
- 623 Melillo, J. M., McGuire, A. D., Kicklighter, D. W., Moore, B., Vorosmarty, C. J., and Schloss, A. L.:  
624 Global climate change and terrestrial net primary production, *Nature*, 363, 234, 10.1038/363234a0, 1993.
- 625 Melillo, J. M., Butler, S., Johnson, J., Mohan, J., Stuedler, P., Lux, H., Burrows, E., Bowles, F., Smith, R.,  
626 Scott, L., Vario, C., Hill, T., Burton, A., Zhou, Y.-M., and Tang, J.: Soil warming, carbon - nitrogen  
627 interactions, and forest carbon budgets, *PNAS*, 108, 9508-9512, 2011.
- 628 Naomi Oreskes, K. S.-F., Kenneth Belitz: Verification, validation, and confirmation of numerical models  
629 in the earth sciences, *Science*, 263, 641-646, 1994.
- 630 O. Skre, W. C. O.: Moss production in a black spruce *Picea mariana* forest with permafrost near  
631 Fairbanks, Alaska, as compared with two permafrost-free stands, *Ecography*, 2, 249-254, 1979.
- 632 Oechel, W. C., Laskowski, C. A., Burba, G., Gioli, B., and Kalhori, A. A. M.: Annual patterns and budget  
633 of CO<sub>2</sub> flux in an Arctic tussock tundra ecosystem, *Journal of Geophysical Research: Biogeosciences*,  
634 119, 323-339, 10.1002/2013jg002431, 2014.
- 635 Okland, R. H.: Population Biology of the Clonal Moss *Hylocomium Splendens* in Norwegian Boreal  
636 Spruce Forests. I. Demography, *Journal of Ecology*, 83, 697-712, 1995.



- 637 P.C. Harley, J. D. T., K.J. Murray, and J. Beyers: Irradiance and temperature effects on photosynthesis of  
638 tussock tundra Sphagnum mosses from the foothills of the Philip Smith Mountains, Alaska, *Oecologia*,  
639 79, 251-259, 1989.
- 640 Pakarinen, P., and D. H. Vitt: Primary production of plant communities of the Truelove Lowland, Devon  
641 Island, Canada–Moss communities, Primary production and production processes, tundra biome.  
642 International Biological Programme, Tundra Biome Steering Committee, Edmonton Oslo, 37-46, 1973.
- 643 Pharo, E. J., and Zartman, C. E.: Bryophytes in a changing landscape: The hierarchical effects of habitat  
644 fragmentation on ecological and evolutionary processes, *Biological Conservation*, 135, 315-325,  
645 10.1016/j.biocon.2006.10.016, 2007.
- 646 Raich, J. W., Rastetter, E. B., Melillo, J. M., Kicklighter, D. W., Steudler, P. A., Peterson, B. J., Grace, A.  
647 L., III, B. M., and Vorosmarty, C. J.: Potential net primary productivity in South America: application of a  
648 global model, *Ecological Applications*, 1, 399-429, 1991.
- 649 Richardson, A. D., Jenkins, J. P., Braswell, B. H., Hollinger, D. Y., Ollinger, S. V., and Smith, M. L.: Use  
650 of digital webcam images to track spring green-up in a deciduous broadleaf forest, *Oecologia*, 152, 323-  
651 334, 10.1007/s00442-006-0657-z, 2007.
- 652 Running, S. W., and Coughlan, J. C.: A general model of forest ecosystem processes for regional  
653 applications I. Hydrologic balance, canopy gas exchange and primary production processes., *Ecological*  
654 *Modelling*, 42, 125-154, 1988.
- 655 S. Frolking, M. L. G., S.C. Wofsy, S-M. Fan, D.J. Sutton, J.W. Munger, A.M. Bazzaz, B.C. Daube, P.M.  
656 Crill, J.D, Aber, L.E. Band, X. Wang, K. Savage, T. Moore And R.C. Harriss: Modelling temporal  
657 variability in the carbon balance of a spruce/moss boreal forest, *Global change biology*, 2, 343-366, 1996.
- 658 Sarah E. Hobbie, J. P. S., Susan E. Trumbore And James R. Randerson: Controls over carbon storage and  
659 turnover in high-latitude soils, *Global change biology*, 6, 196-210, 2000.
- 660 Schimel, D. S., House, J. I., Hibbard, K. A., Bousquet, P., Ciais, P., Peylin, P., Braswell, B. H., Apps, M.  
661 J., Baker, D., Bondeau, A., Canadell, J., Churkina, G., Cramer, W., Denning, A. S., Field, C. B.,  
662 Friedlingstein, P., Goodale, C., Heimann, M., Houghton, R. A., Melillo, J. M., III, B. M., Murdiyarso, D.,  
663 Noble, I., Pacala, S. W., Prentice, I. C., Raupach, M. R., Rayner, P. J., Scholes, R. J., Steffen, W. L., and  
664 Wirth, C.: Recent patterns and mechanisms of carbon exchange by terrestrial ecosystems, *Nature*, 414,  
665 2001.
- 666 Serreze, M. C., and Francis, J. A.: The Arctic on the fast track of change, *Weather*, 61, 65-69, 2006.
- 667 Shetler, G., Turetsky, M. R., Kane, E., and Kasischke, E.: Sphagnum mosses limit total carbon  
668 consumption during fire in Alaskan black spruce forests, *Canadian Journal of Forest Research*, 38, 2328-  
669 2336, 10.1139/x08-057, 2008.



670 Soja, A. J., Tchepakova, N. M., French, N. H. F., Flannigan, M. D., Shugart, H. H., Stocks, B. J.,  
671 Sukhinin, A. I., Parfenova, E. I., Chapin, F. S., and Stackhouse, P. W.: Climate-induced boreal forest  
672 change: Predictions versus current observations, *Global and Planetary Change*, 56, 274-296,  
673 10.1016/j.gloplacha.2006.07.028, 2007.

674 Stow, D. A., Hope, A., McGuire, D., Verbyla, D., Gamon, J., Huemmrich, F., Houston, S., Racine, C.,  
675 Sturm, M., Tape, K., Hinzman, L., Yoshikawa, K., Tweedie, C., Noyle, B., Silapaswan, C., Douglas, D.,  
676 Griffith, B., Jia, G., Epstein, H., Walker, D., Daeschner, S., Petersen, A., Zhou, L., and Myneni, R.:  
677 Remote sensing of vegetation and land-cover change in Arctic Tundra Ecosystems, *Remote Sensing of*  
678 *Environment*, 89, 281-308, 10.1016/j.rse.2003.10.018, 2004.

679 T. G. Williams, L. B. F.: Measuring and modelling environmental influences on photosynthetic gas  
680 exchange in Sphagnum and Pleurozium, *Plant, Cell and Environment*, 21, 555-564, 1998.

681 Tang, J., and Zhuang, Q.: Equifinality in parameterization of process-based biogeochemistry models: A  
682 significant uncertainty source to the estimation of regional carbon dynamics, *Journal of Geophysical*  
683 *Research: Biogeosciences*, 113, 10.1029/2008jg000757, 2008.

684 Tape, K. E. N., Sturm, M., and Racine, C.: The evidence for shrub expansion in Northern Alaska and the  
685 Pan-Arctic, *Global change biology*, 12, 686-702, 10.1111/j.1365-2486.2006.01128.x, 2006.

686 Tarnocai, C., Canadell, J. G., Schuur, E. A. G., Kuhry, P., Mazhitova, G., and Zimov, S.: Soil organic  
687 carbon pools in the northern circumpolar permafrost region, *Global Biogeochemical Cycles*, 23, n/a-n/a,  
688 10.1029/2008gb003327, 2009.

689 Todd-Brown, K. E. O., Randerson, J. T., Post, W. M., Hoffman, F. M., Tarnocai, C., Schuur, E. A. G., and  
690 Allison, S. D.: Causes of variation in soil carbon simulations from CMIP5 Earth system models and  
691 comparison with observations, *Biogeosciences*, 10, 1717-1736, 10.5194/bg-10-1717-2013, 2013.

692 Treseder, K. K., Balser, T. C., Bradford, M. A., Brodie, E. L., Dubinsky, E. A., Eviner, V. T., Hofmockel,  
693 K. S., Lennon, J. T., Levine, U. Y., MacGregor, B. J., Pett-Ridge, J., and Waldrop, M. P.: Integrating  
694 microbial ecology into ecosystem models: challenges and priorities, *Biogeochemistry*, 109, 7-18,  
695 10.1007/s10533-011-9636-5, 2011.

696 Treseder, K. K., Marusenko, Y., Romero-Olivares, A. L., and Maltz, M. R.: Experimental warming alters  
697 potential function of the fungal community in boreal forest, *Global change biology*, 22, 3395-3404,  
698 10.1111/gcb.13238, 2016.

699 Turetsky, M. R., Mack, M. C., Hollingsworth, T. N., and Harden, J. W.: The role of mosses in ecosystem  
700 succession and function in Alaska's boreal forest This article is one of a selection of papers from The  
701 Dynamics of Change in Alaska's Boreal Forests: Resilience and Vulnerability in Response to Climate  
702 Warming, *Canadian Journal of Forest Research*, 40, 1237-1264, 10.1139/x10-072, 2010.



703 Turetsky, M. R., Bond-Lamberty, B., Euskirchen, E., Talbot, J., Froking, S., McGuire, A. D., and Tuittila,  
704 E. S.: The resilience and functional role of moss in boreal and arctic ecosystems, *The New phytologist*,  
705 196, 49-67, 10.1111/j.1469-8137.2012.04254.x, 2012.

706 Wardle, M.-C. N. a. D. A.: Understory vegetation as a forest ecosystem driver: evidence from the northern  
707 Swedish boreal forest, *The Ecological Society of America*, 3, 421–428, 2005.

708 White, A., Cannell, M. G. R., and Friend, A. D.: The high-latitude terrestrial carbon sink: a model analysis  
709 *Global change biology*, 6, 227-245, 2000.

710 Wieder, W. R., Bonan, G. B., and Allison, S. D.: Global soil carbon projections are improved by  
711 modelling microbial processes, *Nature Climate Change*, 3, 909-912, 10.1038/nclimate1951, 2013.

712 Zha, J., and Zhuang, Q.: Microbial decomposition processes and vulnerable Arctic soil organic carbon in  
713 the 21st century, *Biogeosciences Discussions*, 1-34, 10.5194/bg-2018-241, 2018.

714 Zhuang, Q., Romanovsky, V. E., and McGuire, A. D.: Incorporation of a permafrost model into a large-  
715 scale ecosystem model: Evaluation of temporal and spatial scaling issues in simulating soil thermal  
716 dynamics, *Journal of Geophysical Research: Atmospheres*, 106, 33649-33670, 10.1029/2001jd900151,  
717 2001.

718 Zhuang, Q., McGuire, A. D., O'Neill, K. P., Harden, J. W., Romanovsky, V. E., and Yarie, J.: Modeling  
719 soil thermal and carbon dynamics of a fire chronosequence in interior Alaska, *Journal of Geophysical*  
720 *Research*, 108, 10.1029/2001jd001244, 2002.

721 Zhuang, Q., He, J., Lu, Y., Ji, L., Xiao, J., and Luo, T.: Carbon dynamics of terrestrial ecosystems on the  
722 Tibetan Plateau during the 20th century: an analysis with a process-based biogeochemical model, *Global*  
723 *Ecology and Biogeography*, 19, 649-662, 10.1111/j.1466-8238.2010.00559.x, 2010.

724 Zhuang, Q., Chen, M., Xu, K., Tang, J., Saikawa, E., Lu, Y., Melillo, J. M., Prinn, R. G., and McGuire, A.  
725 D.: Response of global soil consumption of atmospheric methane to changes in atmospheric climate and  
726 nitrogen deposition, *Global Biogeochemical Cycles*, 27, 650-663, 10.1002/gbc.20057, 2013.

727 Zhuang, Q., Zhu, X., He, Y., Prigent, C., Melillo, J. M., David McGuire, A., Prinn, R. G., and Kicklighter,  
728 D. W.: Influence of changes in wetland inundation extent on net fluxes of carbon dioxide and methane in  
729 northern high latitudes from 1993 to 2004, *Environmental Research Letters*, 10, 095009, 10.1088/1748-  
730 9326/10/9/095009, 2015.

731  
732  
733  
734



735 **Author contributions.** Q.Z. designed the study. J.Z. conducted model development, simulation  
736 and analysis. J.Z. and Q. Z. wrote the paper.

737 **Competing financial interests.** The submission has no competing financial interests.

738 **Materials & Correspondence.** Correspondence and material requests should be addressed to  
739 qzhuang@purdue.edu.

740

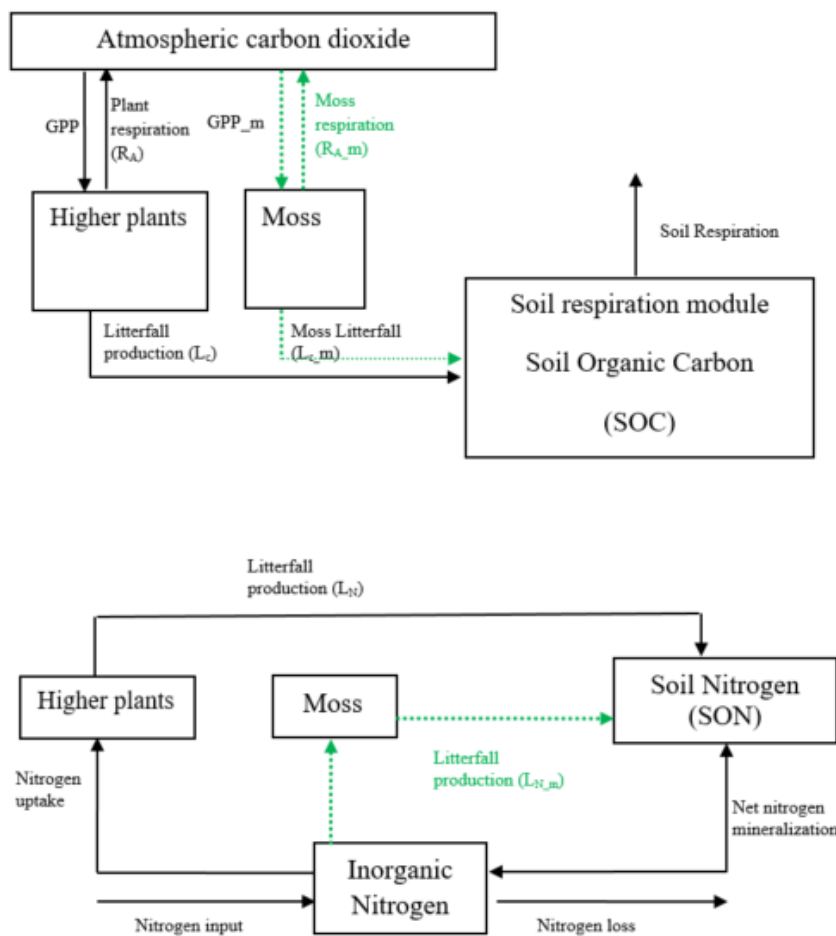
741

742

743

744

745



746

747 Figure 1. Schematic diagram of TEM\_Moss: Green dashed arrows are new carbon and nitrogen  
 748 fluxes, representing moss production, moss respiration and litterfall of moss. Black arrows were  
 749 in TEM 5.0 (Zhuang et al., 2013).

750

751

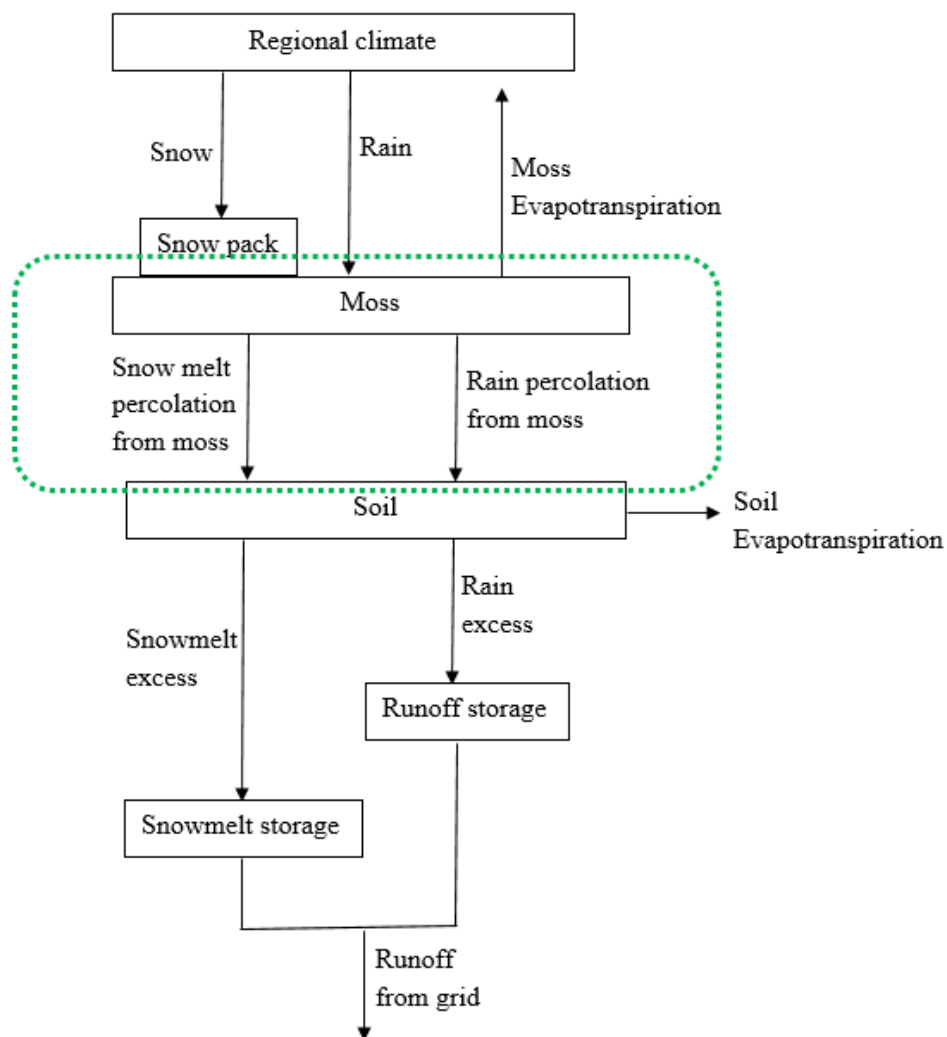
752

753

754

755





756

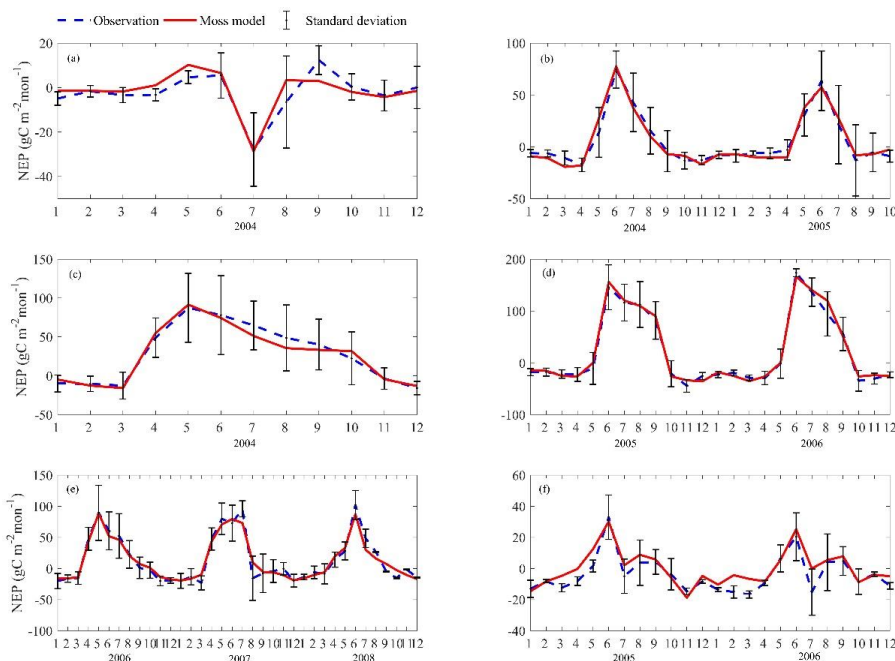
757 Figure 2. The revised Water Balance Model: Green dashed circle represents the hydrology  
758 dynamics for moss (Vörösmarty et al., 1989).

759

760

761

762



763

764 Figure 3. Comparison between observed and simulated NEP ( $\text{gC m}^{-2}\text{mon}^{-1}$ ) at: (a) Ivotuk (alpine  
765 tundra), (b) UCI-1964 burn site (boreal forest), (c) Howland Forest (main tower) (temperate  
766 coniferous forest), (d) Univ. of Mich. Biological Station (Temperate deciduous forest), (e)  
767 KUOM Turfgrass Field (Grassland), and (f) Atqasuk (Wet tundra). Note: scales are different.  
768 Error bars represent standard errors among daily measure data in one month.  
769

770

771

772

773

774

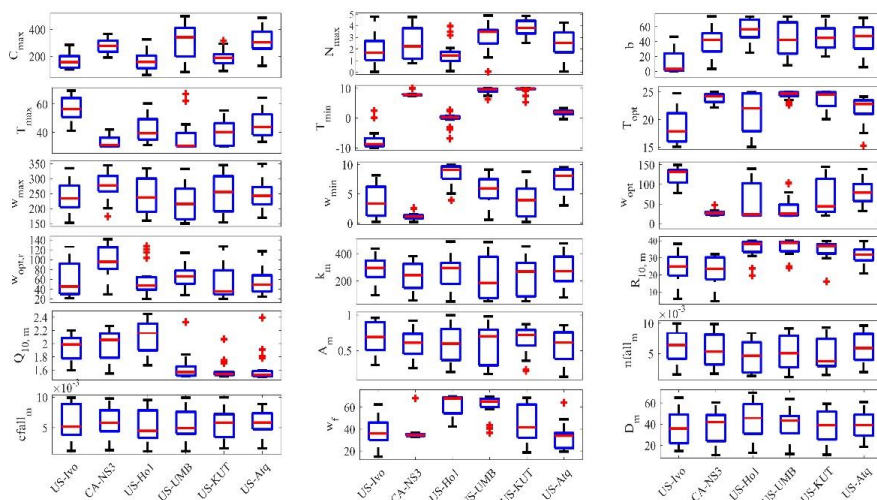
775

776

777

778

779



780

781 Figure 4. Boxplot of parameter posterior distribution that are obtained after ensemble inverse  
 782 modeling for TEM\_Moss all six sites: US-Ivo: Ivotuk (alpine tundra), CA-NS3: UCI-1964 burn  
 783 site (boreal forest), US-Ho1: Howland Forest (temperate coniferous forest), US-UMB: Univ. of  
 784 Mich. Biological Station (temperate deciduous forest), US-KUT: KUOM Turfgrass Field  
 785 (grassland), US-Atq: Atqasuk (wet tundra).

786

787

788

789

790

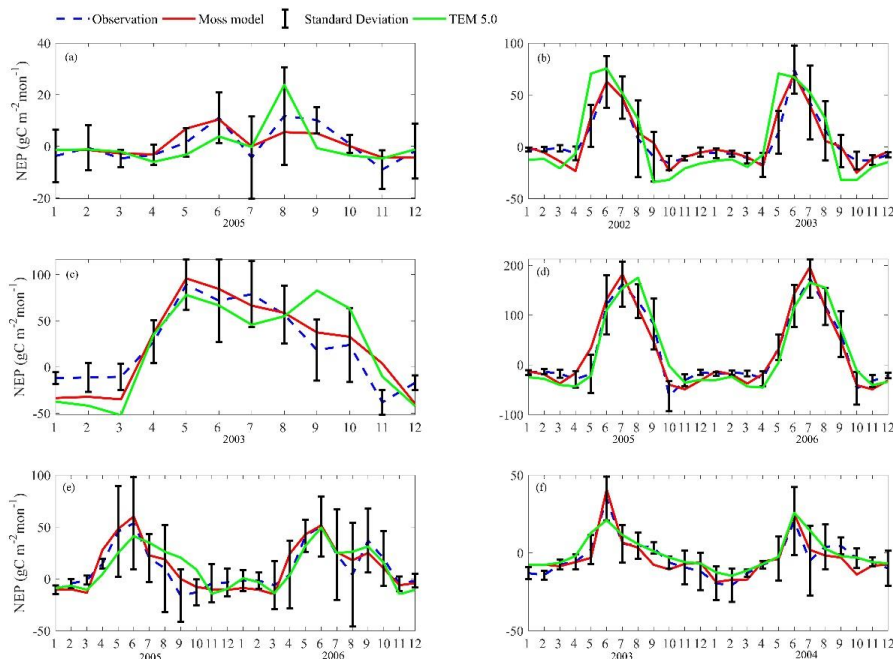
791

792

793

794

795



796

797 Figure 5. Comparison between observed and simulated NEP ( $\text{gC m}^{-2}\text{mon}^{-1}$ ) at: (a) Ivotuk (alpine  
798 tundra), (b) UCI-1964 burn site (boreal forest), (c) Howland Forest (main tower) (temperate  
799 coniferous forest), (d) Bartlett Experimental Forest (Temperate deciduous forest), (e) Brookings  
800 (Grassland), and (f) Atqasuk (Wet tundra). Note: scales are different.

801

802

803

804

805

806

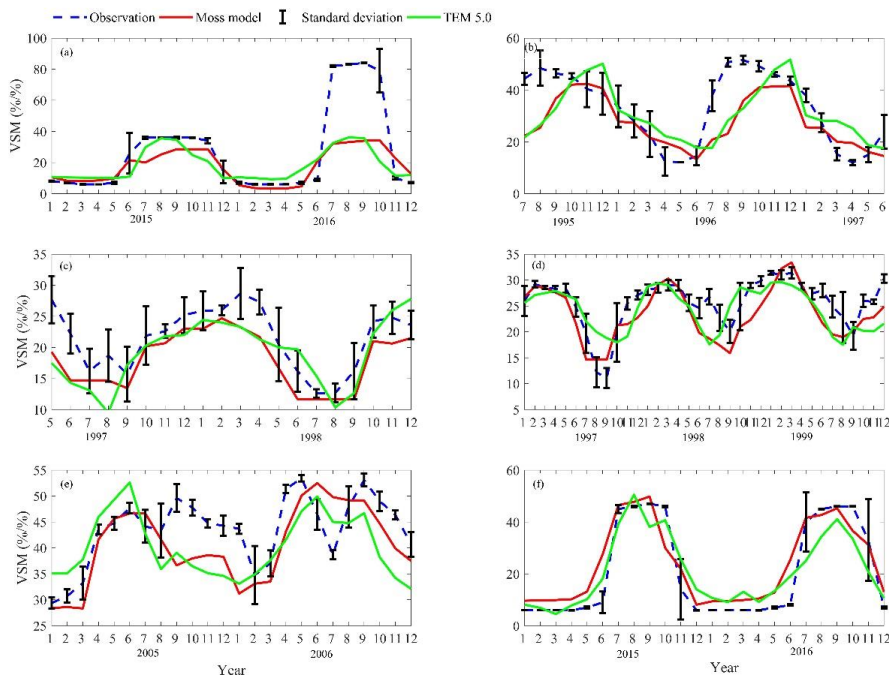
807

808

809

810

811



812

813 Figure 6. Comparison between observed and simulated volumetric soil moisture (VSM, %/%) at:  
814 (a) US-Ivo (alpine tundra), (b) BOREAS NSA-OBS (boreal forest), (c) NL-Loo (temperate  
815 coniferous forest), (d) DK-Sor (Temperate deciduous forest), (e) US-Bkg (Grassland), and (f)  
816 US-Atq (Wet tundra). Note: scales are different.

817

818

819

820

821

822

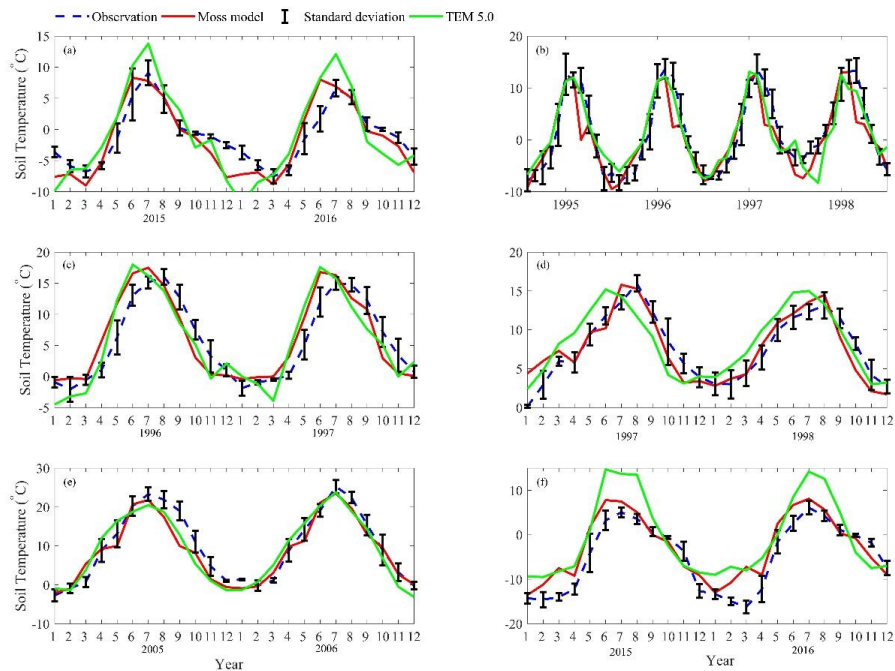
823

824

825

826

827



828  
829 Figure 7. Comparison between observed and simulated soil temperature at 5cm depth (°C) at: (a)  
830 US-Ivo (alpine tundra), (b) BOREAS NSA-OBS (boreal forest), (c) US-Ho1 (temperate  
831 coniferous forest), (d) BE-Vie (Temperate deciduous forest), (e) US-Bkg (Grassland), and (f)  
832 US-Atq (Wet tundra). Note: scales are different.

833

834

835

836

837

838

839

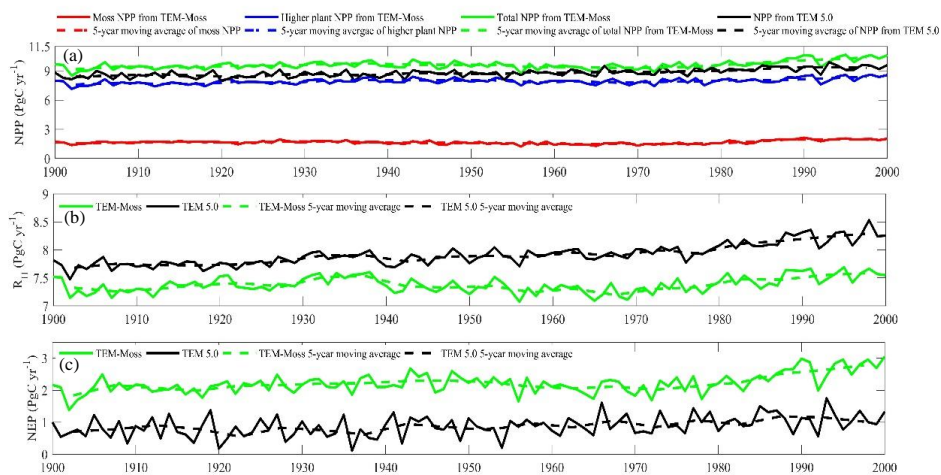
840

841

842

843

844



845

846 Figure 8. Simulated annual net primary production (NPP, a), heterotrophic respiration ( $R_H$ , b),  
847 and net ecosystem production (NEP, c) during the 20<sup>th</sup> century by TEM\_Moss and TEM 5.0.

848

849

850

851

852

853

854

855

856

857

858

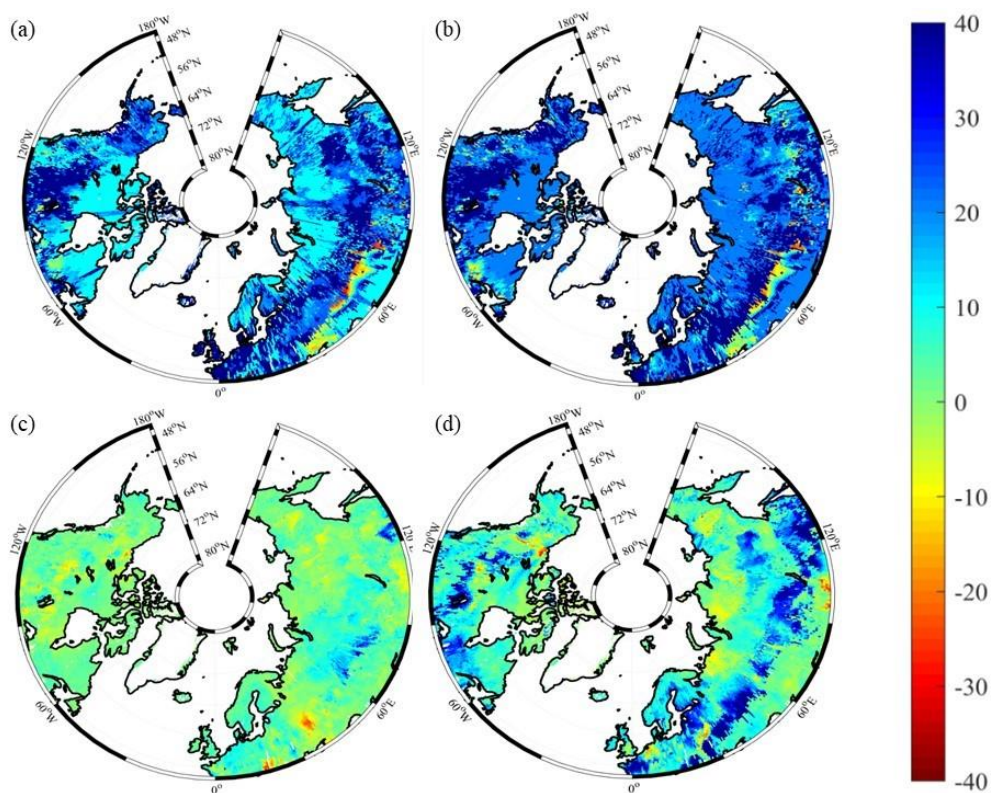
859

860

861

862

863



864

865 Figure 9. Spatial distribution of NEP simulated by TEM\_Moss for the periods (a) 1900–1950, (b)  
866 1951–2000, and by TEM 5.0 for the periods (c) 1900–1950, (d) 1951–2000. Positive values of  
867 NEP represent sinks of CO<sub>2</sub> into terrestrial ecosystems, while negative values represent sources  
868 of CO<sub>2</sub> to the atmosphere.

869

870

871

872

873

874

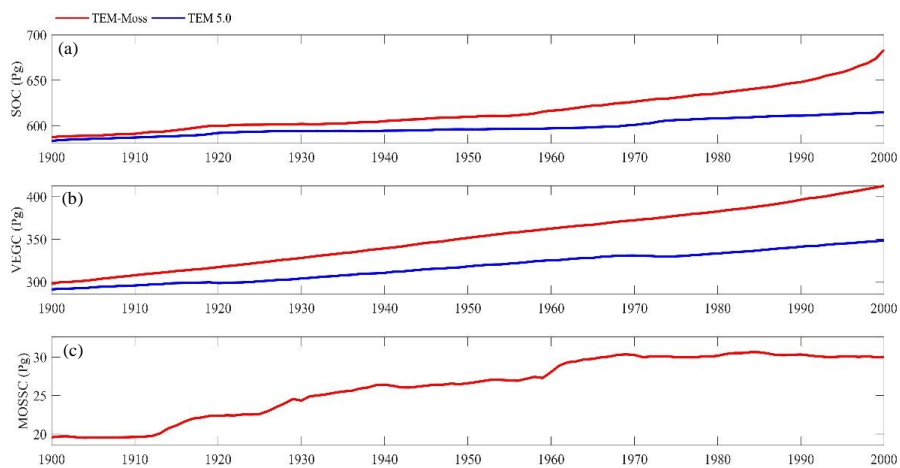
875

876

877

878





879

880 Figure 10. Simulated annual soil organic carbon (SOC, a), vegetation carbon (VEGC, b), and  
881 moss carbon (MOSSC, c) during the 20<sup>th</sup> century by TEM\_Moss and TEM 5.0.

882

883

884

885

886

887

888

889

890

891

892

893

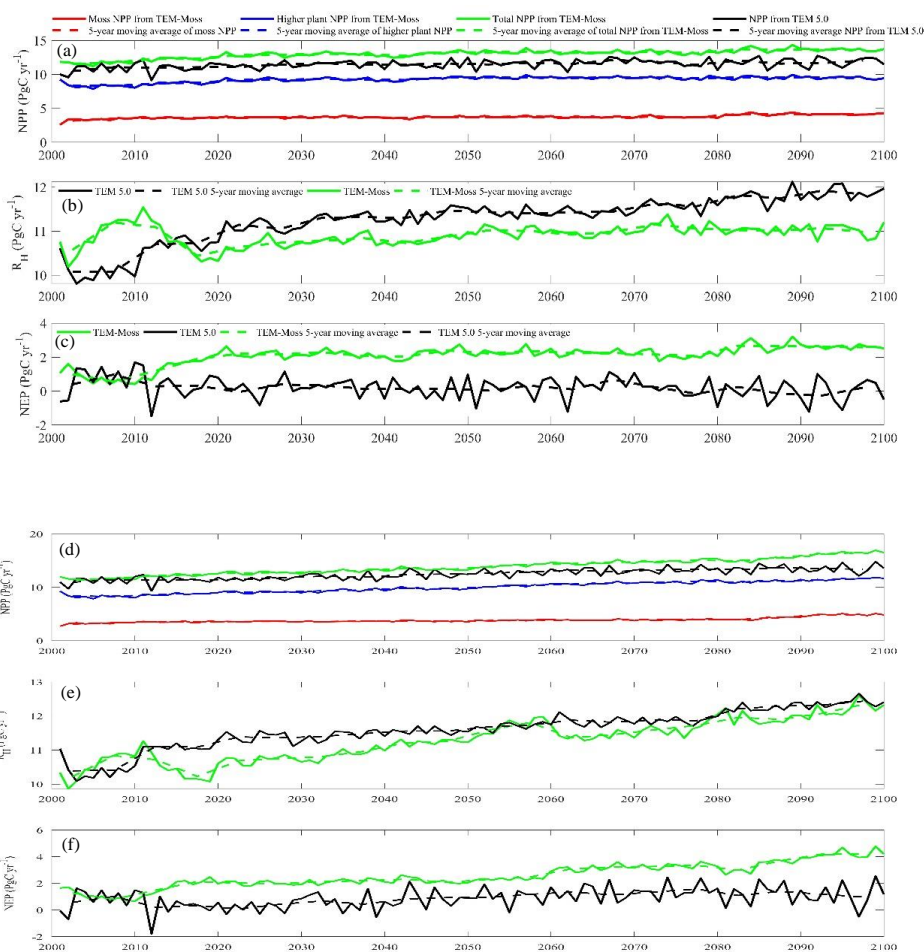
894

895

896

897

898



899

900  
901 Figure 11. Predicted changes in carbon fluxes: annual net primary production (NPP, (a, d)),  
902 heterotrophic respiration ( $R_H$ , (b, e)), and net ecosystem production (NEP, (c, f)) during the 21<sup>st</sup>  
903 century under RCP 2.6 scenario (a, b, c, upper panel) and RCP 8.5 scenario (d, e, f, bottom  
904 panel) by TEM\_Moss and TEM 5.0.

905

906

907

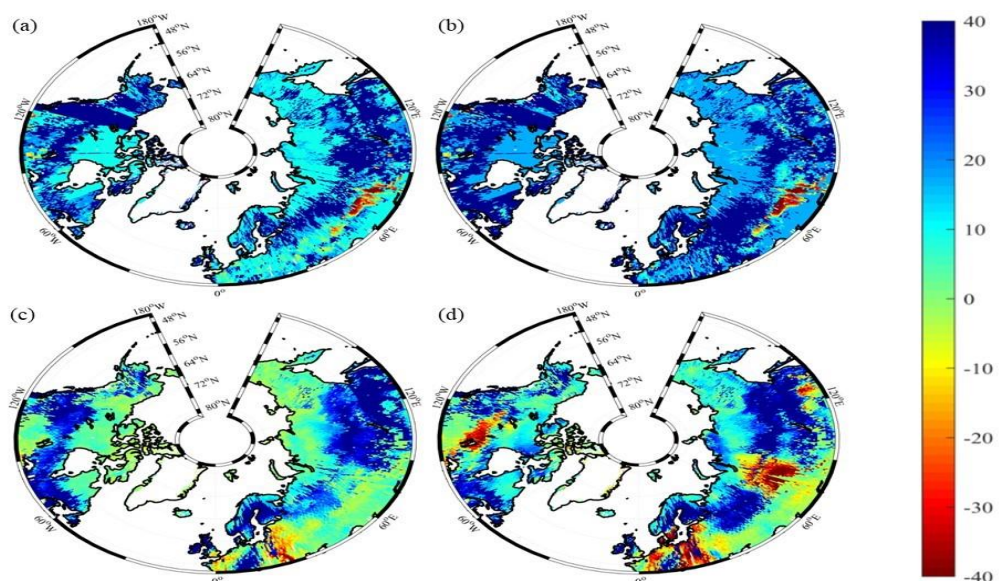
908

909

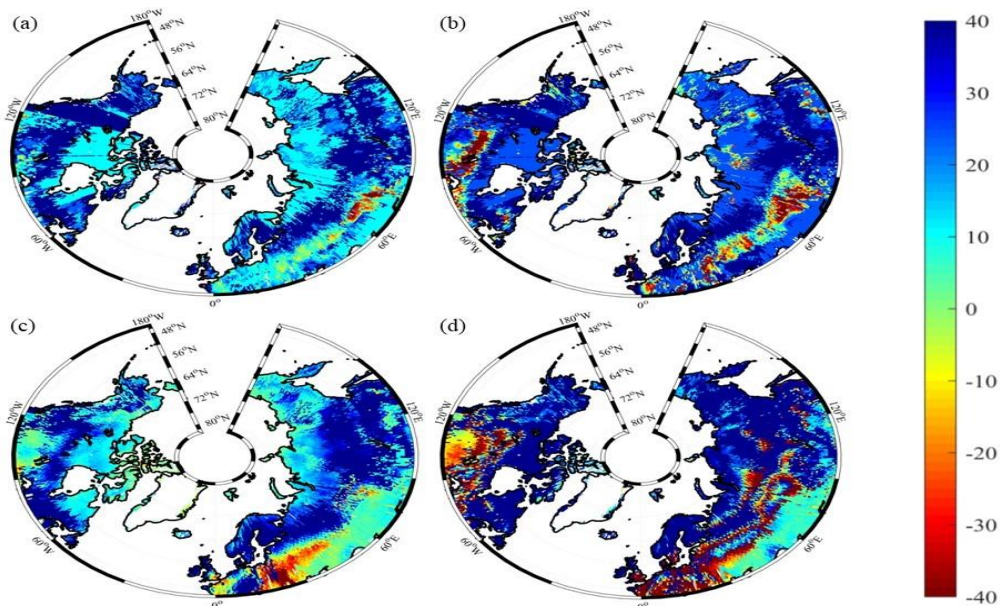
910



911



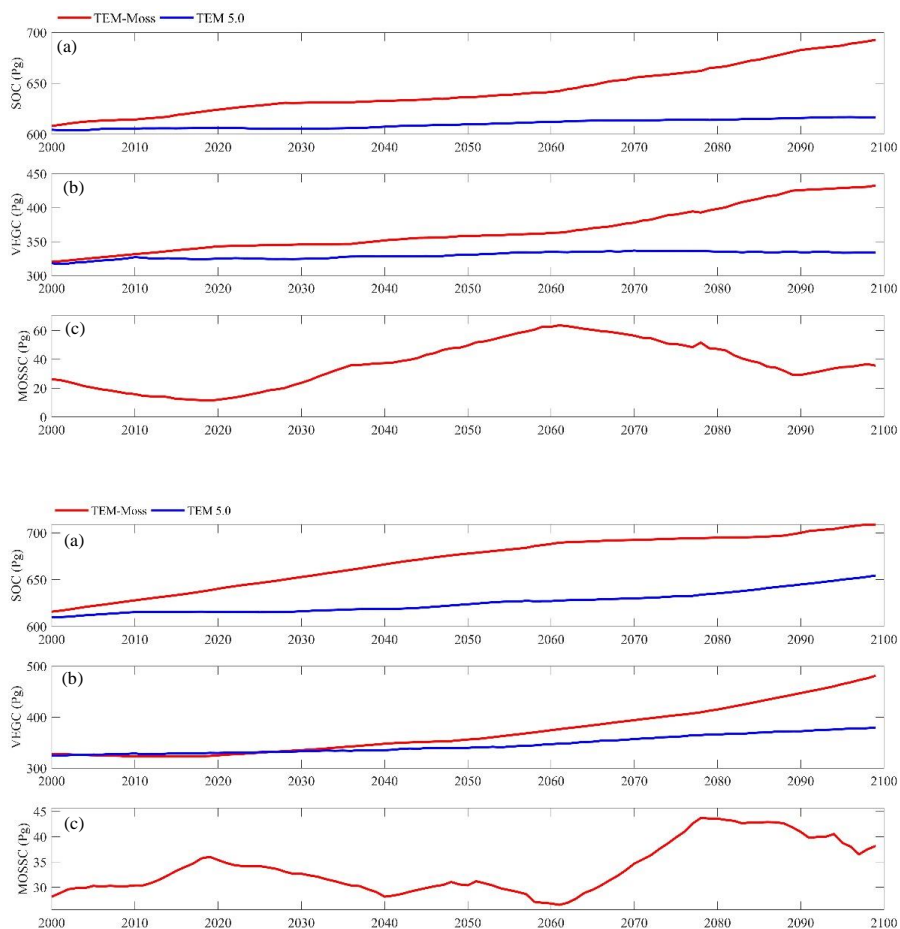
912



913

914 Figure 12. Spatial distribution of NEP simulated for the periods (a) 2000–2050, (b) 2051–2099  
915 by TEM\_Moss, and by TEM 5.0 (c, d) during the 21<sup>st</sup> century under RCP 2.6 scenario (upper  
916 panel) and RCP 8.5 scenario (bottom panel). Positive values of NEP represent sinks of CO<sub>2</sub> into  
917 terrestrial ecosystems, while negative values represent sources of CO<sub>2</sub> to the atmosphere.

918



919

920

921 Figure 13. Simulated annual soil organic carbon (SOC, a), vegetation carbon (VEGC, b), and  
922 moss carbon (MOSSC, c) during the 21<sup>st</sup> century by TEM\_Moss and TEM 5.0 under RCP 2.6  
923 scenario (upper panel) and RCP 8.5 scenario (bottom panel).

924

925

926

927

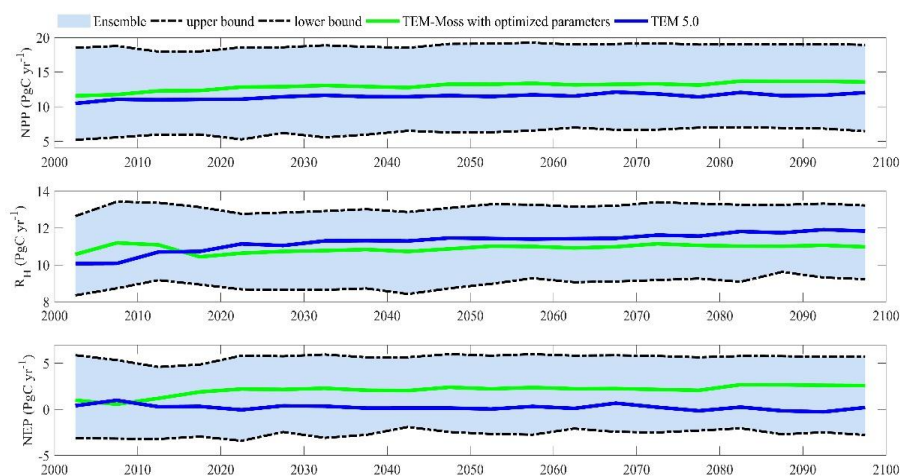
928

929

930

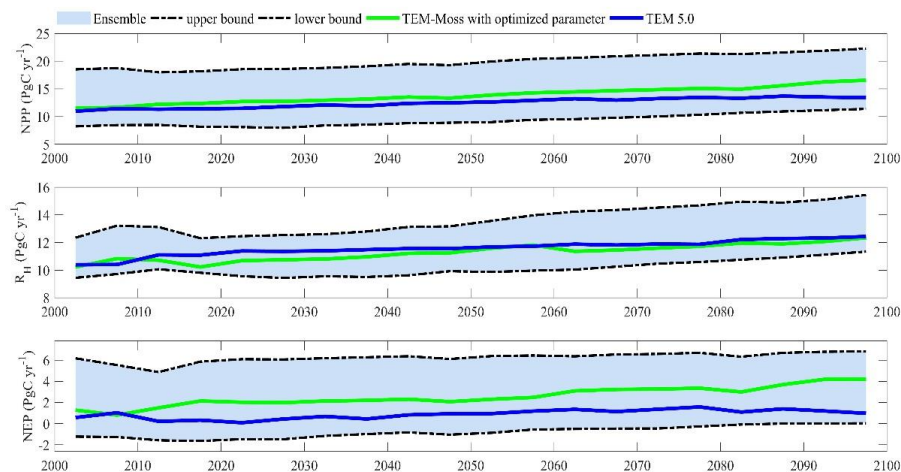


931 (a)



932

933 (b)



934

935 Figure 14. 5-year moving average plots for carbon fluxes under the (a) RCP 2.6 scenario and (b)  
936 RCP 8.5 scenario. The blue area represents the upper and lower bounds of simulations.

937

938

939



940 **Table 1. Parameters associated with moss activities in TEM\_Moss**

Parameters	Units	descriptions	Parameter range (value)	references
$C_{max}$	$gC\ m^{-2}\ mon^{-1}$	maximum rate of C assimilation	[50,500]	Launiainen et al. (2015); Williams & Flanagan (1998)
$b$	$\mu mol\ m^{-2}\ s^{-1}$	Light half-saturation level	[5, 150]	Launiainen et al. (2015); Raich et al. (1991)
$T_{min}$	$^{\circ}C$	minimum temperature	[-10, 10]	Frolking et al. (1996); Raich et al. (1991)
$T_{max}$	$^{\circ}C$	maximum temperature	[30, 80]	Frolking et al. (1996); Raich et al. (1991)
$T_{opt}$	$^{\circ}C$	optimal temperature	[15, 30]	Frolking et al. (1996); Raich et al. (1991)
$w_{min}$	mm	minimum water content for moss photosynthesis	[0.5, 15]	Frolking et al. (1996); Launiainen et al. (2015)
$w_{max}$	mm	maximum water content for moss photosynthesis	[150, 380]	Frolking et al. (1996); Launiainen et al. (2015)
$w_{opt}$	mm	optimal water content for moss photosynthesis	[10, 150]	Frolking et al. (1996); Zhuang et al. (2002)
$k_m$	$\mu L/L$	$CO_2$ concentration half-saturation level	[50, 500]	Zhuang et al. (2002); Raich et al. (1991)
$R_{10, m}$	$gC\ m^{-2}\ mon^{-1}$	moss respiration rate at 10 $^{\circ}C$	[0,40]	Frolking et al. (1996); Launiainen et al. (2015)
$Q_{10, m}$	-	moss respiration temperature sensitivity	[1.5, 2.5]	Frolking et al. (1996); Launiainen et al. (2015)
$w_{opt, r}$	mm	optimal water content for moss respiration	[10, 150]	Frolking et al., 1996; Zhuang et al. (2002)
$c_{fall, m}$	$g^{-1}g^{-1}\ mon^{-1}$	constant proportion for carbon litterfall from moss	[0.001, 0.01]	Zhuang et al. (2002); Raich et al. (1991)
$N_{max}$	$gN\ m^{-2}\ mon^{-1}$	maximum rate of N uptake by mosses	[0.1,5]	Zhuang et al. (2002); Raich et al. (1991)
$k_n$	$g\ m^{-2}$	Half-saturation constant for N uptake by moss	1.0	Zhuang et al. (2002); Raich et al. (1991)
$A_m$	-	relative allocation of effort to C vs. N uptake	[0,1]	Raich et al. (1991)
$w_f$	mm	moss field capacity	[10, 80]	Frolking et al. (1996); Raich et al. (1991)
$n_{fall, m}$	$g^{-1}g^{-1}\ mon^{-1}$	constant proportion for nitrogen litterfall from moss	[0.001, 0.01]	Zhuang et al. (2002); Raich et al. (1991)
$D_m$	mm	Moss thickness	[0, 100]	Zhuang et al. (2002)



**Table 2. Site description and measured NEP data used to calibrate TEM\_Moss**

Site Name	Location (Longitude (degrees) /Latitude (degrees))	Elevation (m)	Vegetation type	Description	Data range	Citations
Univ. of Mich. Biological Station	84.71W 45.56 N	234	Temperate deciduous forest	Located within a protected forest owned by the University of Michigan. Mean annual temperature is 5.83°C with mean annual precipitation of 803mm	01/2005- 12/2006	Gough et al. (2013)
Howland Forest (main tower)	68.74W 45.20N	60	Temperate coniferous forest	Closed coniferous forest, minimal disturbance.	01/2004- 12/2004	Davidson et al. (2006)
UCI-1964 burn site	98.38W 55.91N	260	Boreal forest	Located in a continental boreal forest, dominated by black spruce trees, within the BOREAS northern study area in central Manitoba, Canada.	01/2004- 10/2005	Goulden et al. (2006)
KUOM Turfgrass Field	93.19W 45.0N	301	Grassland	A low-maintenance lawn consisting of cool-season turfgrasses.	01/2006- 12/2008	Hiller et al. (2010)
Atkasuk	157.41W 70.47N	15	Wet tundra	100 km south of Barrow, Alaska. Variety of moist-wet coastal sedge tundra, and moist-tussock tundra surfaces in the more well-drained upland.	01/2005- 12/2006	Oechel et al. (2014);
Ivotuk	155.75W 68.49N	568	Alpine tundra	300 km south of Barrow and is located at the foothill of the Brooks Range and is classified as tussock sedge, dwarf-shrub, moss tundra.	01/2004- 12/2004	McEwing et al. (2015)



**Table 3. Site description and measured NEP data used to validate TEM\_Moss**

Site Name	Location (Longitude (degrees) /Latitude (degrees))	Elevation (m)	Vegetation type	Description	Data range	Citations
Bartlett Experimental Forest	71.29W/ 44.06N	272	Temperate deciduous forest	Located within the White Mountains National Forest in north-central New Hampshire, USA, with mean annual temperature of 5.61 °C and mean annual precipitation of 1246mm.	01/2005- 12/2006	Jenkins et al. (2007); Richardson et al. (2007);
Howland Forest (main tower)	68.74W/ 45.20N	60	Temperate coniferous forest	Closed coniferous forest, minimal disturbance.	01/2003- 12/2003	Davidson et al. (2006)
UCI-1964 burn site	98.38W/ 55.91N	260	Boreal forest	Located in a continental boreal forest, dominated by black spruce trees, within the BOREAS northern study area in central Manitoba, Canada.	01/2002- 12/2003	Goulden et al. (2006)
Brookings	96.84W/ 44.35N	510	Grassland	Located in a private pasture, belonging to the Northern Great Plains Rangelands, the grassland is representative of many in the north central United States, with seasonal winter conditions and a wet growing season.	01/2005- 12/2006	Gilmanov et al. (2005)
Atkasuk	157.41W/ 70.47N	15	Wet tundra	100 km south of Barrow, Alaska. Variety of moist-wet coastal sedge tundra, and moist-tussock tundra surfaces in the more well-drained upland.	01/2003- 12/2004	Oechel et al. (2014);
Ivotuk	155.75W/ 68.49N	568	Alpine tundra	300 km south of Barrow and is located at the foothill of the Brooks Range and is classified as tussock sedge, dwarf-shrub, moss tundra.	01/2005- 12/2005	McEwing et al. (2015)





**Table 4. Site description and measured volumetric soil moisture data used to validate TEM\_Moss**

Site	Location (Longitude (degrees) /Latitude (degrees))	Elevation (m)	Vegetation type	Data range	Citations
US-Ivo	155.75W/ 68.49N	579	Alpine tundra	01/2015- 12/2016	Oechel & Kalhori (2018)
BOREAS NSA-OBS	98.48W/ 55.88N	259	Boreal forest	07/1995- 06/1997	Stangel & Kelly (1999)
NL-Loo	5.74E/ 52.17N	25	Temperate coniferous forest	05/1997- 12/1998	Falge et al. (2005)
DK-Sor	11.64E/ 55.49N	40	Temperate deciduous forest	01/1997- 12/1999	Falge et al. (2005)
US-Bkg	96.84W/ 44.35N	510	Grasslands	01/2005- 12/2006	Gilmanov et al. (2005)
US-Atq	157.41W/ 70.47N	25	Wet tundra	01/2015- 12/2016	Oechel & Kalhori (2018)



**Table 5. Site description and measured soil temperature at 5cm depth data used to validate TEM\_Moss**

Site	Location (Longitude (degrees) /Latitude (degrees))	Elevation (m)	Vegetation type	Data range	Citations
US-Ivo	155.75W/ 68.49N	579	Alpine tundra	01/2015- 12/2016	Oechel & Kalhori (2018)
BOREAS NSA-OBS	98.48W/ 55.88N	259	Boreal forest	01/1995- 12/1998	Stangel & Kelly (1999)
US-Ho1	68.74W/ 45.2N	60	Temperate coniferous forest	01/1996- 12/1997	Falge et al. (2005)
BE-Vie	6.0E/ 50.3N	493	Temperate deciduous forest	01/1997- 12/1998	Falge et al. (2005)
US-Bkg	96.84W/ 44.35N	510	Grasslands	01/2005- 12/2006	Gilmanov et al. (2005)
US-Atq	157.41W/ 70.47N	25	Wet tundra	01/2015- 12/2016	Oechel & Kalhori (2018)



**Table 6. Model validation statistics for TEM\_Moss and TEM 5.0 at six sites with NEP data**

Site Name	Vegetation type	Models	Intercept	Slope	R-square	Adjusted R-square	RMSE	p-value
Ivotuk	Alpine tundra	TEM_Moss	0.46	0.61	0.72	0.70	3.57	<0.001
		TEM 5.0	-0.22	0.75	0.43	0.41	5.88	0.02
UCI-1964 burn site	Boreal forest	TEM_Moss	-0.13	1.01	0.91	0.90	8.33	<0.001
		TEM 5.0	-2.45	1.29	0.75	0.74	20.1	<0.001
Howland Forest (main tower)	Temperate coniferous forest	TEM_Moss	-1.28	1.05	0.83	0.81	19.69	<0.001
		TEM 5.0	-2.22	0.97	0.62	0.61	31.23	0.002
Bartlett Experimental Forest	Temperate deciduous forest	TEM_Moss	-0.49	1.03	0.94	0.94	19.06	<0.001
		TEM 5.0	-2.49	1.04	0.91	0.89	23	<0.001
Brookings	Grassland	TEM_Moss	0.36	1.02	0.85	0.84	8.95	<0.001
		TEM 5.0	2.58	0.75	0.62	0.6	13.07	<0.001
Atqasuk	Wet tundra	TEM_Moss	-0.36	0.97	0.84	0.83	5.13	<0.001
		TEM 5.0	1.99	0.75	0.75	0.74	6.56	<0.001



**Table 7. Model validation statistics for TEM\_Moss and TEM 5.0 at six sites with volumetric soil moisture data**

Site ID	Vegetation type	Models	Intercept	Slope	R-square	Adjusted R-square	RMSE	p-value
US-Ivo	Alpine tundra	TEM_Moss	8.56	0.34	0.74	0.72	20.8	<0.001
		TEM 5.0	10.67	0.29	0.64	0.62	21.76	<0.001
BOREAS NSA-OBS	Boreal forest	TEM_Moss	10.71	0.51	0.52	0.51	11.1	<0.001
		TEM 5.0	16.47	0.43	0.32	0.31	11.96	<0.001
NL-Loo	Temperate coniferous forest	TEM_Moss	0.47	0.82	0.83	0.81	4.0	<0.001
		TEM 5.0	3.75	0.72	0.49	0.48	4.5	<0.001
DK-Sor	Temperate deciduous forest	TEM_Moss	1.39	0.86	0.67	0.65	3.65	<0.001
		TEM 5.0	10.41	0.54	0.4	0.39	4.06	<0.001
US-Bkg	Grassland	TEM_Moss	5.64	0.8	0.51	0.49	6.05	<0.001
		TEM 5.0	22.24	0.41	0.21	0.2	7.34	0.027
US-Atq	Wet tundra	TEM_Moss	7.76	0.77	0.87	0.85	7.38	<0.001
		TEM 5.0	6.74	0.68	0.85	0.84	7.63	<0.001



**Table 8. Model validation statistics for TEM\_Moss and TEM 5.0 at six sites with soil temperature at 5cm depth data**

Site ID	Vegetation type	Models	Intercept	Slope	R-square	Adjusted R-square	RMSE	p-value
US-Ivo	Alpine tundra	TEM_Moss	-0.34	1.16	0.83	0.82	2.54	<0.001
		TEM 5.0	0.54	1.36	0.75	0.73	3.94	<0.001
BOREAS NSA-OBS	Boreal forest	TEM_Moss	-0.05	0.91	0.9	0.88	2.24	<0.001
		TEM 5.0	0.27	0.81	0.84	0.82	2.9	<0.001
US-HoI	Temperate coniferous forest	TEM_Moss	0.7	0.95	0.81	0.79	2.93	<0.001
		TEM 5.0	-0.06	0.99	0.77	0.76	3.41	<0.001
BE-Vie	Temperate deciduous forest	TEM_Moss	0.57	0.92	0.83	0.81	1.82	<0.001
		TEM 5.0	1.88	0.85	0.69	0.68	2.56	<0.001
US-Bkg	Grassland	TEM_Moss	0.17	0.87	0.91	0.89	2.87	<0.001
		TEM 5.0	-0.01	0.91	0.89	0.87	3.04	<0.001
US-Atq	Wet tundra	TEM_Moss	1.36	0.86	0.84	0.82	3.63	<0.001
		TEM 5.0	4.33	0.99	0.75	0.74	6.17	<0.001



**Table 9.** Average annual NPP,  $R_H$  and NEP (as Pg C per year) during the 20<sup>th</sup> century estimated by two models.

Average annual carbon fluxes (PgC yr <sup>-1</sup> )	TEM_Moss	TEM 5.0	Difference	Moss NPP/ Higher plant NPP
Moss NPP	1.69	-	-	21.3%
Higher plant NPP	7.93	8.8	-	
Total NPP	9.6	8.8	0.8	
$R_H$	7.38	7.91	-0.53	
NEP	2.22	0.89	1.33	



**Table 10. Increasing of SOC, vegetation carbon (VGC), and moss carbon (MOSSC) from 1900 to 2000, and total carbon storage during the 20<sup>th</sup> century predicted by two models.**

Models	Carbon pools	Carbon pool amounts in 1900/2000 (units: Pg)	Changes in carbon pools during the 20 <sup>th</sup> century (units: Pg)
TEM_Moss	SOC	587.1/683.4	96.3
	VEGC	297.5/412.7	115.2
	MOSSC	19.6/30	10.4
	Total	904.2/1126.1	221.9
TEM 5.0	SOC	583.2/614.9	31.7
	VEGC	291.1/348.6	57.5
	Total	874.3/963.5	89.2



**Table 11. Average annual NPP,  $R_H$  and NEP (as Pg C per year) during the 21<sup>st</sup> century estimated by two models under (a) RCP 8.5 scenario and (b) RCP 2.6 scenario.**

		TEM_Moss	TEM 5.0	Difference	Moss NPP/ Higher plant NPP
<b>(a)</b>	Average annual carbon fluxes (PgC yr <sup>-1</sup> )				
	Moss NPP	3.84	-	-	38.4%
	Higher plant NPP	10	12.53	-	
	Total NPP	13.84	12.53	1.31	
	$R_H$	11.28	11.54	-0.21	
	NEP	2.56	0.99	1.57	
<b>(b)</b>					
<b>(b)</b>	Average annual carbon fluxes (PgC yr <sup>-1</sup> )				Moss NPP/ Higher plant NPP
	Moss NPP	3.74	-	-	40.5%
	Higher plant NPP	9.24	11.52	-	
	Total NPP	12.98	11.52	1.46	
	$R_H$	10.91	11.24	-0.33	
	NEP	2.07	0.28	1.79	





**Table 12. Increasing of SOC, vegetation carbon (VGC), and moss carbon (MOSSC) from 1900 to 2000, and total carbon storage during the 21<sup>st</sup> century predicted by two models under (a) RCP 2.6 scenario and (b) RCP 8.5 scenario.**

(a)

Models	Carbon pools	Carbon pool amounts in 2000/2099 (units: Pg)	Changes in carbon pools during the 21 <sup>st</sup> century (units: Pg)
TEM_Moss	SOC	608.1/692.8	84.7
	VEGC	320.2/432.8	112.6
	MOSSC	26.2/35.6	9.4
	Total	954.5/1161.2	206.7
TEM 5.0	SOC	604.4/616.5	12.1
	VEGC	318.2/333.7	15.5
	Total	922.6/950.2	27.6

(b)

Models	Carbon pools	Carbon pool amounts in 2000/2099 (units: Pg)	Changes in carbon pools during the 21 <sup>st</sup> century (units: Pg)
TEM_Moss	SOC	615.9/708.4	92.5
	VEGC	327.8/481.4	153.6
	MOSSC	28.1/38.2	10.1
	Total	971.8/1228.0	256.2
TEM 5.0	SOC	610.2/654.4	44.2
	VEGC	324.9/379.4	54.5
	Total	935.1/1033.8	98.7